Multivalency associated properties of polysulfated nanomaterials in biomedical applications

Dissertation zur Erlangung des akademischen Grades des
Doktors der Naturwissenschaften (Dr. rer. nat.)

eingereicht im Fachbereich Biologie, Chemie, Pharmazie
der Freien Universität Berlin

vorgelegt von

Jonathan Vonnemann

aus Dortmund

November 2014

Diese Arbeit wurde unter der Anleitung von Prof. Dr. Rainer Haag im Zeitraum von November 2010 bis November 2014 am Institut für Chemie und Biochemie der Freien Universität Berlin angefertigt.

1. Gutachter: Prof. Dr. Rainer Haag

2. Gutachter: PD Dr. Christoph Böttcher

Disputation am 19. Dezember 2014

Acknowledgements

First of all I would like to thank Prof. Dr. Rainer Haag for giving me the opportunity to work in his group. His financial and scientific support of my project as well as his unfailing confidence in me in the form of simple kindnesses and encouragement were very much appreciated. Furthermore, I am very grateful to PD Dr. Christoph Böttcher whose accuracy and persistence have produced lasting scientific results. Having him scrutinize my projects has been a painful but at the same time highly enjoyable and rewarding process. I am glad and thankful to have him as the second reviewer of this thesis. Jutta Hass and Dr. Pamela Winchester deserve special thanks for helping me with bureaucratic "challenges," proofreading, and for extensive discussions about the English language, in which I finally always had to capitulate. Many thanks also go to all present and former members of our group. In no particular order I would like to thank Dr. Dominic Gröger, Benjamin Ziem, Dr. Carlo Fasting, Wei Qiang, Dr. Marie Weinhart, Olaf Wagner, Dr. Katja Neuthe, Virgina Wycisk, and Cathleen Schlesener for supporting me on numerous occasions. I would also be remiss if I did not thank my colleague and good friend Tobias Becherer, who has accompanied me with support and fruitful discussions since my Masters.

Furthermore, I would like to cordially thank all of my past and present cooperation partners, Dr. Jens Dernedde, Dr. Sebastian Riese, Dr. Katharina Achazi, Dr. Stefanie Wedepohl, and Christian Kühne. It has always been a pleasure to work and spend time with you. Thank you for the countless hours of SPR measurements and instrumental instructions. My sincere thanks also go to Dr. Kai Ludwig and Andrea Schulz; I really enjoyed my time spent in your department. Furthermore, I would like to acknowledge Dr. Nicolas Bezière, Prof. Dr. Andreas Herrmann, and Dr. Christian Sieben for the excellent corporations which enabled this highly interdisciplinary work. Furthermore, special thanks go to Susanne Liese, who was able to put my thoughts into mathematical equations. If you ever need a mathematician, I would highly commend her. I also acknowledge the analytical department at the FU Berlin for their kind support. Finally, I am grateful to my family and friends for their support and encouragement.

In particular I want to thank my own little family, Deborah and Apolline, for their patience and support.

Contents

1. Introduction

Nanomaterials can be found in all areas of science and applications including electronics,[1] diagnostics,[2] nanomedicine[3] and cosmetics.[4] The high applicability of nanomaterials can be ascribed to the vast number of possible modifications that can be performed on the nanomaterials, all leading to unique properties. Especially the core of inorganic nanoparticles already inherently contains useful functions like fluorescence, magnetism, UV-Vis absorption, conductivity, and degradability, depending on the material, size, and shape of the nanoscopic object. Furthermore, nanomaterials offer a large surface area which additionally can be functionalized by a variation of targeting ligands, drugs, and signaling moieties. Hence, the field of nanomedicine has particularly been growing, as the combined properties of the nanoparticular core as well as ligand functionalization offer numerous ways to vary the biological interaction. Additionally, as nanoparticles bridge the gap between the size of molecules and biological objects (Figure 1), functional nanomaterials can be used to investigate the biological activity of molecules on virus- and cell-like dimensions.

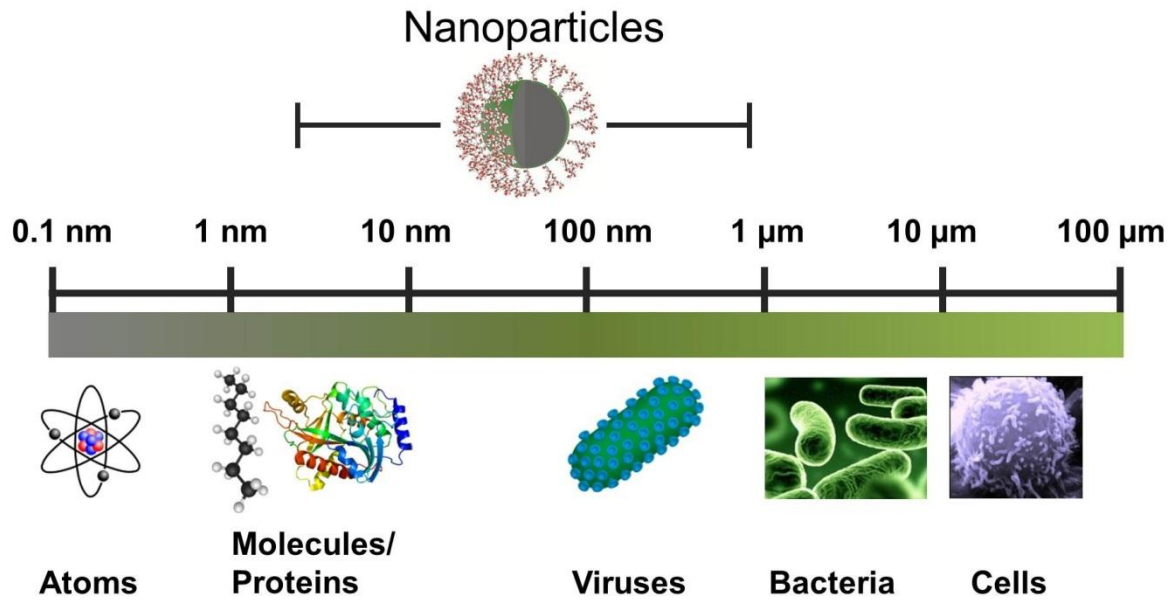

Figure 1. Length scale of chemical and biological entities.

Nevertheless, nanotechnology is still in an embryonic state application-wise, partly because of the elusive interactions of nanomaterials with biological systems. One example is the influence of multivalency effects, in other words, the influence of multiple ligand/receptor interactions, on the binding affinity of nanomaterials to biological membranes. Nature employs this mechanism

abundantly, as the binding of viruses, bacteria, and leucocytes to endothelial cells is in all cases associated with large contact areas and therefore, multiple interactions. In many cases, the properties of a new molecule are only investigated in its monomolecular form but not in its multivalently presented form on size scales larger than 20 nm. One example is dendritic polyglycerolsulfate (dPGS), which was reported by our group 10 years ago and proved to be a highly potent entity in the field of nanomedicine. dPGS is a synthetic analog of heparin which permits the imaging and therapy of inflammatory diseases and has the potential to inhibit viral infections, whereby many of its biological functions are based on multivalent interactions. Nevertheless, so far, the largest dPGS that could be synthesized was 17 nm in diameter and thus significantly smaller than the approximately 100 nm sized viruses or even micrometer sized bacteria or cells (Figure 1). The work of my thesis focuses on combining the biological active properties of dPGS with virus-sized gold nanostructures for the targeting of inflammatory diseases and the inhibition of viral infections. By the systematic variation of the core size and shape, my aim is to get deeper insight into the impact of multivalency on binding events at virus-like dimensions and to employ this knowledge for the preparation of highly potent virus inhibitors and nanodiagnostics for inflammatory processes, respectively.

1.1 Multivalency and binding inhibition

In order to identify requirements for the preparation of highly potent virus inhibitors and nanodiagnostics based on multivalency effects, I will briefly outline the concept of multivalency.

The human body is a highly complex and self-organized system which consists of an immense number of components and fine-tuned interactions. Therefore, it is not surprising that nature employs all kinds of principles to control the binding strength and reversibility of biological components with a minimum amount of synthetic effort. As exemplified on the influence virus, multivalency is one of nature`s key principles to achieve this goal. The adhesion of the influenza virus to the host cell before endocytotic uptake is primarily mediated by the interaction of the trimeric lectin hemagglutinin (HA) on the viral surface and the tetrasaccharide sialyl-Lewis^X (sLe^X),[5] which is abundantly present in the cellular glycocalyx.[6] Not only one copy of HA is incorporated in the viral protein layer, but a total of 600-1200 copies/virus,[5] therefore several HA/sLe^X interactions simultaneously take place when the virus comes in contact with the cell. As a result, the multivalent binding energy is much larger than the binding energy of a single HA/sLe^X interaction. The magnitude of the multivalent binding energy is primarily dependent on the number of multiple monovalent binding events (*N*), which itself is restricted by the contact area of the virus with the cell. By varying the size, shape, or ligand density of a biological object, nature can smoothly regulate its affinity to extreme magnitudes; even by using the same ligand/receptor pair over and over again.[5] Another specific property of multivalency is the reversibility of the binding. Since each individual bond within the multivalent binding process is relatively weak, a directional or constant force will break the individual ligand/receptor bonds one by one. Therefore, in contrast to a single very strong bond, multivalent binding events are reversible. Nature employs this property, for example, in the leucocyte recruitment cascade as discussed in detail in Chapter 1.2.1.[7] Before transmigration, leukocytes bind multivalently to the inflamed endothelium by multiple interactions of cell adhesion molecules (CAMs) and their corresponding receptors.[7] The density of CAMs presented on the endothelium, as well as the larger contact area because of the deformation of the leucocyte upon adhesion, regulate the number of individual interactions and supplies nature with another continuous regulation of the number of transmigrating leukocytes and, as a result, of the level of inflammation.[7] Besides the impact of multivalency on biological binding events, it also is also a key requirement for many cellular signal transduction pathways.[8] As my thesis is concerned with the binding of polysulfated nanostructures to biological surfaces, I will focus on the former.

1.1.1 Definition and quantification of multivalency

The concept of multivalency is also well known in other chemical sciences, even though it is often differently labeled.[9] For example, the concept of chelation introduced by Schwarzenbach and coworkers in the 1950s is conceptually very closely related to multivalency.[10] The binding properties of immunoglobulins depending on their valency, which is commonly described as avidity, serves as another example (the exact origin of the term avidity is unknown). While the principle of avidity and chelating usually copes with situations of $N < 10$, the concept of multivalency also covers higher valent interactions ($N > 10$), as often observed in biological binding events, i.e., the binding of viruses to cells. These types of multivalent interactions are usually called polyvalent interactions.[5] Polyvalency is therefore a subunit of multivalency. Nevertheless, as the number of ligand/receptor pair interactions in the experimental work of this thesis was in many cases unknown, I will employ the term multivalency throughout, even if the binding events are assumably often associated with $N > 10$. The multivalent enhancement of the free energy of binding (ΔG) and therefore binding constant (K) is usually quantified by the following equations (Eq. 1, 2).[5]

$$\Delta G_N^{multi} = N\Delta G_{avg}^{multi} = \alpha N \Delta G_N^{multi} \qquad \text{(Eq. 1)}$$

$$K_N^{multi} = (K_{avg}^{multi})^N = (K^{mono})^{\alpha N} \qquad \text{(Eq. 2)}$$

The superscript *multi* and *mono* describe the multivalent and monovalent presentation of the ligand, while the subscript N or *avg* defines the sum or average of all binding events, respectively. The cooperativity factor α quantifies the effect of the multivalent presentation on each individual binding event.[11] It also serves as a basis for defining multivalent systems into positively cooperative ($\alpha > 1$), non-cooperative ($\alpha = 1$), and negative cooperative ($\alpha < 1$) systems.[5] The determination or even the quantification of the cooperativity has mostly been performed so far on lower valent systems in which N could be predefined synthetically.[12,13] Whether a multivalent system is positively or negatively cooperative dependence on a large number of factors which are excellently presented in a recent review by Fasting et al.[9] Briefly, the important factors which influence the cooperativity of a system are (1) the changes in the solvation, translational and rotational entropies of each individual ligand and the scaffold and (2) the changes in the binding enthalpy of each individual ligand within the multivalent binding process. Additionally, the scaffold itself can have a major effect on the multivalent binding energy because of interactions with the receptor. As a result, identifying these effects and the type of cooperativity is a tedious process and usually requires a vast combination of experiments and simulations. Nevertheless, these studies are essential, as they pave the way for the implementation of multivalency as a design principle for high affinity binders. The most important element in the design

of multivalent binders is of course the scaffold upon which the ligands are attached. In order to benefit from multivalency, the scaffold is required to provide a ligand spacing large enough to facilitate the maximum number of ligand/receptor interactions. This can often only be achieved by using flexible spacers like linear polymers. Flexible spacers, on the other hand, lose more degrees of freedom and thus entropy upon multivalent binding which lowers the overall binding energy.[9] Hence, the best spacers are highly rigid with a ligand spacing just high enough to facilitate all the multiple ligand-receptor interactions.[9] The identification of cooperativity effects gets increasingly difficult for higher valent systems like viruses or ligand functionalized nanoparticles. First of all, these systems are usually too large for many *in silica* approaches like molecular modeling and for many experimental techniques like NMR or MS.[13,14] As a result, most investigations on the multivalent interactions of these systems are based on techniques which benefit from the large mass and density of the scaffold (SPR/QCM),[15] the high contrast (TEM/DLS),[16,17] or on specific physical properties of inorganic cores like fluorescence or UV-Vis absorption.[18] Nevertheless, the biggest problem in the identification of cooperativity for systems with higher valency is the lack of knowledge about the actual number of multiple binding ligand/receptor pairs *N*. Despite the significant challenges associated with identifying the degree of the system's cooperativity, it is important to keep in mind that a multivalent presentation of ligands is in most cases still advantageous for application, even for non- or negatively cooperative systems.[5] Hence, Whitesides and coworkers have proposed that the multivalent enhancement of these systems should be quantified by the enhancement factor β (Eq. 3).[5]

$$\beta = \frac{K_N^{multi}}{K^{mono}} \qquad \text{(Eq. 3)}$$

In the literature, enhancement factors β of even up to several million have been observed.[5] Nevertheless, the exact properties of an entity which influence β are still elusive and systematic studies that enable the prediction of the multivalent binding constants of colloids are overdue.

1.1.2 Multivalency in competitive binding inhibition

Due to the significant challenges associated with the quantification of multivalency for higher valent systems, over the last few decades, research has been mainly focused on optimizing multivalent systems for application.[19] The main reasons for preparing multivalent systems for biomedical applications are (1) to achieve very high binding constants for targeted therapeutics or diagnostics and (2) to design highly efficient viral or bacterial inhibitors. As a major part of my thesis focuses on the development and understanding of multivalent virus inhibitors, I will examine the latter aspect in more detail. The efficacy of a multivalent binding inhibitor is usually quantified by the level of its concentration required to achieve half-maximum inhibition (IC_{50}). The IC_{50} values of binding

inhibitors are usually assessed by competitive binding inhibition assays. These kinds of assays generally consist of the binder, i.e., virus, which binding to a ligand functionalized target surface, i.e., cells, is desired to be inhibited (Figure 2).

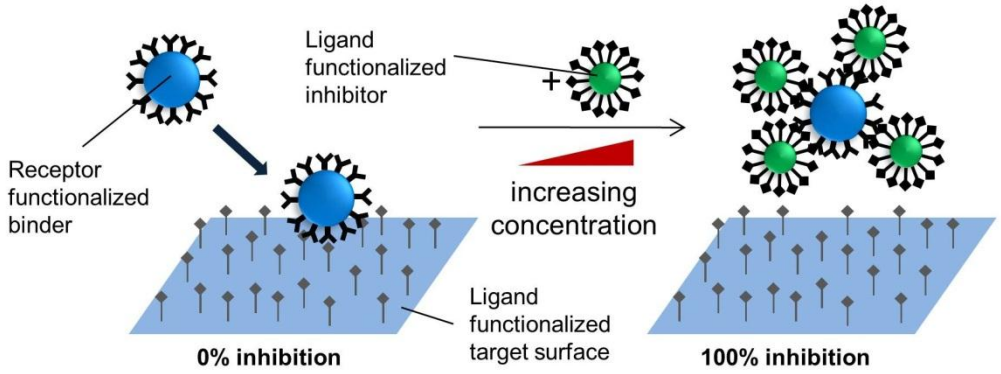

Figure 2. Schematic presentation of a typical competitive binding assay. The number of binding events if there is no inhibitor is usually referred to as 0% inhibition. Upon increasing the inhibitor concentration, fewer binders attach to the ligand functionalized surface due to a competitive binding of the inhibitors to the binders.

The nomenclature within the field is inconsistent. In virology, it is widely accepted that the binding entities on the virus and on the host cell are termed ligands and receptors, respectively. In the field of competitive binding inhibitors, however, the attention is focused on the binding of the inhibitor to the binder. Therefore Whitesides and coworkers, who started this field, termed the binding entities on the inhibitor and binder ligand and receptor, respectively.[5] As this thesis focuses on the evaluation of competitive binding inhibitors, the latter nomenclature was adopted. For determining IC_{50} values, the assays depicted in Figure 2 are most suited if the binder's attachment to the target surface results in a quantifiable signal. A good example of this type of assay is the SPR based competitive binding assay as established in the group of Dernedde and coworkers.[20–23] This assay was also widely employed in the experimental work of this thesis. A special type of competitive binding inhibition assay is the hemagglutination inhibition assay,[24] which is widely employed in the field of virology. Since it does not have a quantifiable read-out, the lowest concentration of inhibitor for inhibiting agglutination is usually employed for comparison. The binders in this assay are in most cases virions, while the functionalized surface is represented by the red blood cells. As red blood cells are at least one order of magnitude bigger than the virions (Figure 1), the surface of the red blood cells can be assumed to be essentially planar. In order to obtain IC_{50} values from competitive binding inhibition assays, the binders are generally preincubated with the inhibitors which results in a concentration dependent reduction of the measurement signal (Figure 2). As all IC_{50} values of competitive binding inhibitors in

literature are based on this procedure, it is even more important to understand the requirements for the comparison of data obtained by these assays. In the end, comparable IC_{50} values will be needed to identify design principles for more optimal inhibitors. The IC_{50} values from separately performed assays are only comparable under strict application of the same assay parameters, an aspect which is often neglected. Therefore, in order to interpret the effect of multivalent presentation of ligands on the binding inhibition, the IC_{50} values of multivalent inhibitors and the monovalent ligand would need to be compared. As a multivalent presentation of ligands is often only desired because the monovalent ligand is a very weak binder in the first place, the monovalent IC_{50} cannot always be determined experimentally. This further complicates the comparability of IC_{50} values between different assays. Nevertheless, IC_{50} values of multivalent inhibitors measured within the same assay provide a direct comparison of their inhibition potential and, as a result, can be used for optimization of the respective type of inhibitor.

The most investigated binder for multivalent binding inhibitors is, by far, the influenza virus which makes it a prime example for surveying the influence of the employed multivalent scaffold on the inhibition potential.[17,25–32] I will hereby only focus on larger, highly multivalent systems that can bind to several HA units on the virus instead of lower valent systems, which are optimized for the binding of a single HA trimer,[33] even though they might be more efficient for application (Chapter 1.2.3). The field of multivalently presented sialic acid (SA) groups for the inhibition of influenza was started by the group of Whitesides in 1993 when it was discovered that the incorporation of SA functionalized ganglosides into liposomes significantly lowered the required concentrations of ganglosides to inhibit influenza induced agglutination.[25] The enhanced inhibitory effect was thought to be based on a higher binding affinity because of multivalency effects, nevertheless, the capability of the liposomal scaffold to block additional receptors on the virus due to steric shielding of the liposome, which at that point was called steric occlusion, was yet unknown. Hence, it was not possible to give a statement on the contribution of multivalency. Over the last 20 years, attempts to quantify this ”steric shielding” effect on competitive binding inhibition have been unsuccessful, which has prohibited the elucidation of mechanism underlying competitive binding inhibition. Therefore, a major part of my thesis focuses on quantifying this effect. The list of scaffolds for the multivalent presentation of sialic acid groups has been meanwhile constantly growing and now includes linear polymers,[27,29,30] dendrimers,[34,35] liposomes,[25] polymersomes,[31] nanogels,[28] and nanoparticles.[17,36] An excellent recent review by Bhatia et al. summarizes some recent advances in multivalent glycoconjugates as possible antiviral agents.[37] Despite the immense synthetic effort put into developing these multivalent SA based inhibitors, a general principal for the design of an optimal virus inhibitor is still overdue. The first conclusive results concerning the mechanism for competitive binding inhibition were produced in the lab of Whitesides and his coworkers, which were concerned with linear, sialic acid functionalized polyacrylamides.[27,29,30] Whitesides showed in his first study that the inhibition potential of polymeric

fragments with different molecular weights of 10-2000 kDa correlated with their binding affinity, which itself significantly increased for higher molecular weight polymers.[30] These results already proved that the binding of the inhibitor is a major prerequisite for inhibition and that this binding was enhanced by multivalency. The mechanism of inhibition was assumed to be not only based on the occupation of the HA binding pockets but also on the steric shielding of the virus due to the volume each chain occupied on the virus. In a follow-up study, this effect was more closely examined in inhibition experiments of linear, SA functionalized linear polymers in the presence of monomeric neuraminidase (NA) inhibitors.[29] The addition of NA inhibitors increased the inhibitory potential of the SA functionalized polymeric inhibitors, which was assumed to be based on a less compact conformation of the SA polymers on the virus and thus higher steric shielding. Similar to the first study, the quantification of this steric shielding effect and correlation with molecular properties was not possible. This was the last known attempt in the literature to quantify the effect of steric shielding on binding inhibition. Focusing on another property of the inhibitor, Whitesides also investigated the dependence of the binding inhibition on the degree of sialic acid functionalization.[27] It was observed that the degree of functionalization had an impact on the inhibitory potential of the polymer, whereby Whitesides introduced a new way to normalize the inhibition data. As previously discussed, the enhancement of binding affinities by multivalency effects is usually quantified by the relation of the multivalent binding constant to the number of ligand/receptor interactions *N* (Eq. 2). Possibly as a result, Whitesides normalized the inhibition data according to the overall concentration of ligand moieties, i.e., SA groups and not based on the concentration of inhibitors, i.e., SA functionalized polymers. For more than twenty years now, the scientific community has adopted this type of data interpretation for multivalent inhibitors which has resulted in very low IC_{50} values per SA group down to the low nanomolar range.[5,27–30] Nevertheless, neither the actual mass normalized efficacy of the multivalent inhibitors nor the origin of these very low IC_{50} values per sialic acid groups could be sufficiently discussed. The challenge in quantifying multivalency from inhibition data is the lack of quantitative data about steric shielding, which itself is likely to be dependent on the size and geometry of the employed scaffold. As this further complicates a comparison of different inhibitors, no solution for the approach of this problem is currently available. Within the scope of this thesis, I will attempt to establish a model systems based on dPGS functionalized nanomaterials in order to optimize the current approach of interpreting inhibition results. Additionally, my goal is to quantify the contributions of multivalency and steric shielding effects to competitive binding inhibition for enabling a rational design of competitive binding inhibitors.

1.2 Polysulfates and their biological interactions

For the evaluation of dPGS functionalized nanostructures as multivalent inhibitors in biomedical applications, a detailed understanding of the interaction of polyanions with physiological components is required. In this chapter I will give a general overview about the interaction of polyanions within the body and then focus on the application of polysulfates as anti-viral and anti-inflammatory compounds, respectively.

The biological interactions of polycations and polyanions can be generalized to some extent. Polycations are generally known to be more toxic than polyanions,[38] as their electrostatic attraction to the negatively charged cell membrane can result in lysis of the cell membrane.[39] Nevertheless, the strong interaction with the cellular membrane enhances the endocytotic uptake.[40] Therefore, polycations can facilitate the transfer of drugs or nanoparticles into the cytoplasm.[41] The positive charge can further be employed for complexation with polyanions like RNA or DNA for transfectional therapy.[40] Most cationic compounds employed for biomedical applications are based on amine groups, as they also enhance the endosomal escape of polyplexes.[38,40,41] The concrete cause for the enhanced endosomal escape of polyamines is still elusive.[42] In contrast to polycations, polyanions are known to be less toxic.[38] Polyanions carry the same surface charge as the cellular membrane and the glycocalyx and thus interact weaker with cellular surfaces. The anionic groups present within the body are quite varying with carboxyls, phosphates, phosphonates, sulfates, and sulfonates. Interestingly, when multivalently presented, these groups specifically bind to different biological surfaces. For example, phosponates and phosphates can be employed for targeting bone,[43] while polysulfates show enhanced specificity to viruses and targets involved in inflammatory processes.[44,45] The following sections will discuss the synthesis of polysulfates and their application as anti-inflammatory agents and virus targeting moiety.

1.2.1 Anti-inflammatory properties of polysulfates

The first step of an inflammatory process is the recruitment of leucocytes into the inflamed tissue, a process commonly known as the leucocyte recruitment cascade.[7] The leucocyte recruitment cascade is a complex process involving vasodilation and the expression of chemokines, cytokines, and various cell-adhesion molecules (CAMs) for the chemotactical attraction as well as binding of leucocytes.[7] The initial capture of the leucocytes from the blood flow is based on the interactions of the glycoprotein L-selectin on the leucocytes with its respective ligand PSGL-1 on the inflamed endothelium.[7,46] One of the major interactions of all three selectins, namely, P-, E-, and L-selectin, is driven by a calcium mediated protein-carbohydrate interaction of the selectins with sLe^X on the

respective ligand.[7] The first fully characterized physiological ligand which binds to all three selectins was the human P-selectin glycoprotein ligand 1 (PSGL-1) (Figure 3).[47]

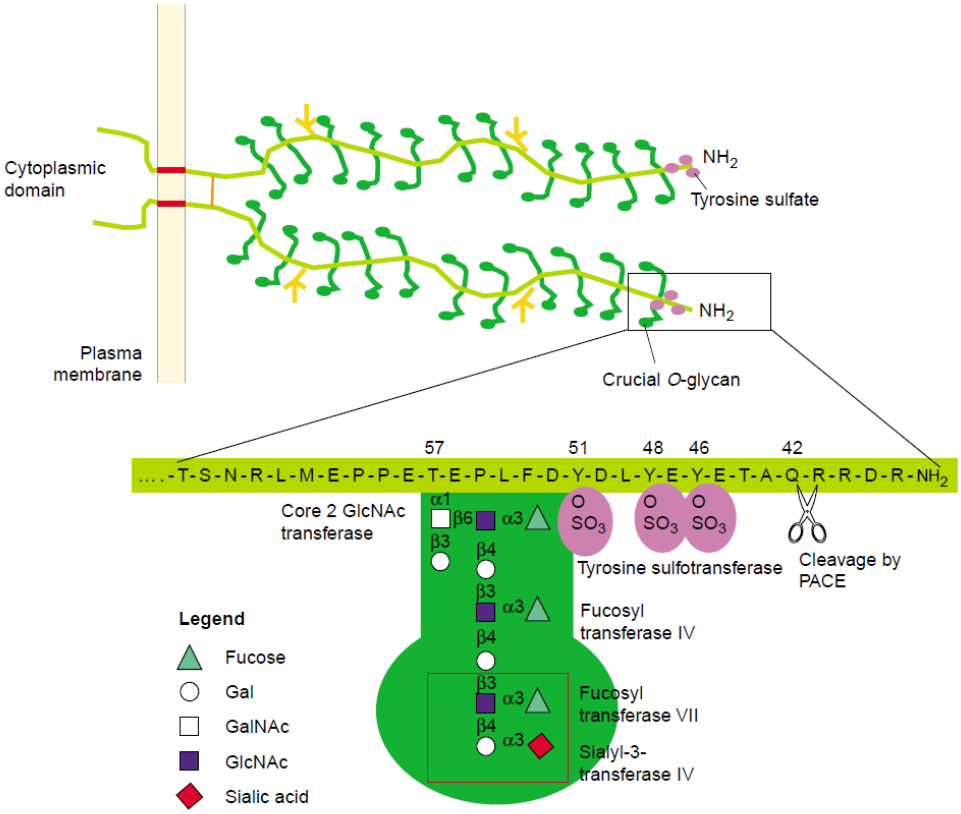

Figure 3. Structure of the human P-selectin glycoprotein ligand 1 (PSGL-1) homodimer, which is the major physiological ligand for selectins. Printed with permission from Ley et al.[47] Copyright 2003 Elsevier. The tyrosine sulfate groups (marked in purple) at the NH_2-terminus were found to be highly involved in the binding of L- and P-selectin.[48,49]

The most important structural part for the selectin binding activity is located at the NH_2-terminus (Figure 3, black box), which is associated with N-terminal tyrosine sulfates (purple) and the minimal selectin recognition motif, sLe^x (Figure 3, red box).[47] Interestingly, the tyrosine sulfates in PSGL-1 were shown to be essential for binding to P- and L-selectin[48,49] but not to E-selectin.[50] These results not only imply that the essential structure for binding E-selectin and P-, L-selectin may differ respectively, but they also suggest that sulfates play an important role in the binding activity of P- and L-selectin. There are several examples which fortify this hypothesis. Another major cell adhesion molecular (CAM), called glycosylation-dependent cell adhesion molecule-1 (GlyCAM-1) can bind to all three selectins.[51] Intensive studies on the posttranslational modifications of GlyCAM-1 have shown that sulfation of the oligosaccharide side chains is essential for L-selectin binding,[52] which could be confirmed by recent electrostatic energy computations.[53] Furthermore, heparin and other natural sulfated polysaccharides not only show anti-coagulant and anti-complementary activities but

also exhibit high affinity to P- and L-selectins with IC_{50} values in the low micromolar range, despite the lack of the sLe^x binding domain.[44] Nevertheless, even though the multivalent presentation of sulfate groups on heparin results in very high binding affinities to selectins, heparin has to be extracted from mammalian organs which is cost-intensive and can result in contamination with prions. In combination with the strong anti-coagulant properties of heparin, its application as anti-inflammatory agent is very limited. Therefore, our group has prepared dendritic polyglycerolsulfate (dPGS) as a new anti-inflammatory polyanionic entity which only marginally effects on the blood coagulation.

1.2.1.1 dPGS – a new anti-inflammatory polyanion

Polysulfates have a high potential for targeting and treating inflammatory processes.[44] According to this concept the Haag group sulfated polyglycerol (PG), which turned out to be a highly effective anti-inflammatory agent. The core of it consists of PG, which is a highly biocompatible and multivalent scaffold, ranging from nano- to micrometers (Figure 4).[54]

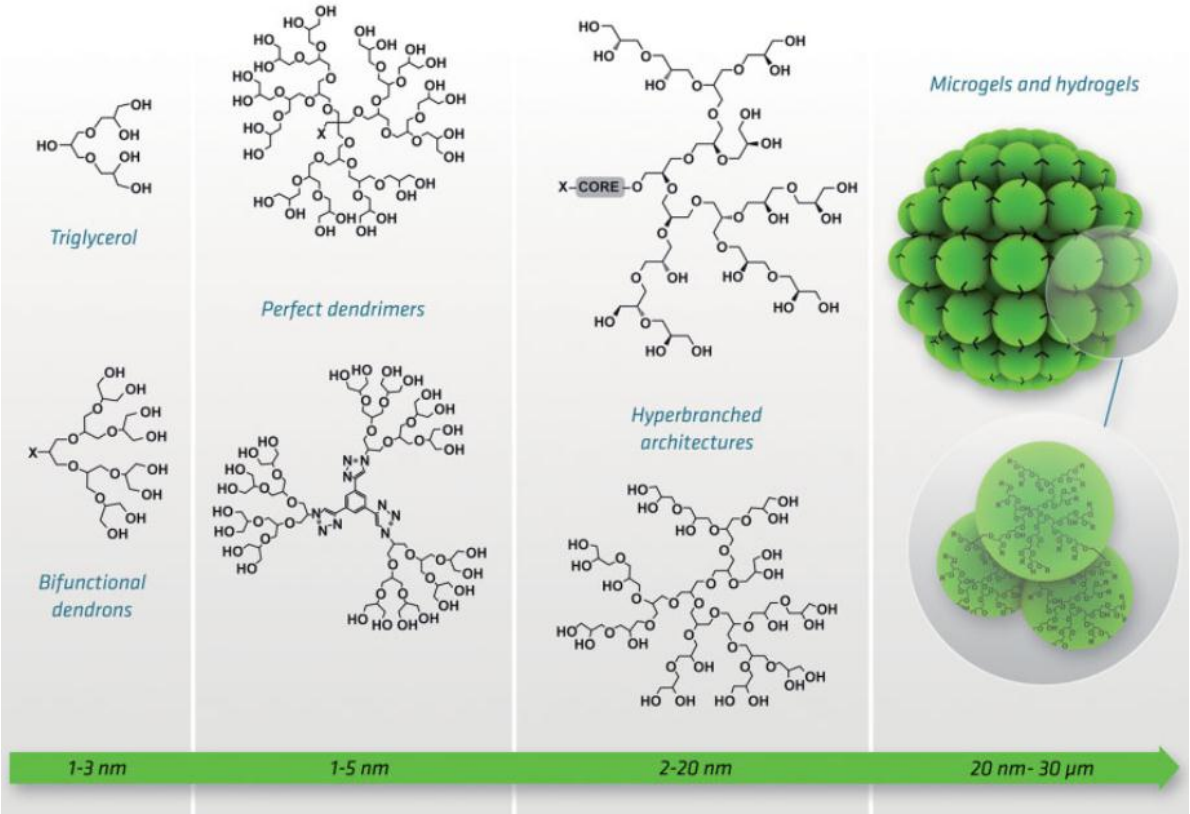

Figure 4. Library of synthetic polyglycerols of various dimensions for biomedical applications. Used with permission from Calderón et al.[54] Copyright 2010 Wiley.

Because of its excellent solubility in water and low toxicity, polyglycerol is a highly suitable scaffold for biomedical applications.[54] Brooks and coworkers reported similar or even better biocompatibility profiles for dendritic polyglycerols than for polyethylene glycol (PEG) with a molecular weight (MW) of 4.2 and 670 kDa.[54,55] Furthermore, branched polyglycerols have an exceptionally high plasma half-life and exhibit higher thermal and oxidative stability than PEG.[56] In contrast to PEG, PG has a large amount of free hydroxyl groups at the periphery, which permits a great variety of possible functionalizations.[54] Considering the biocompatibility and tunable dimension, it is of no surprise that dendritic polyglycerol has found its way into a vast number of applications like drug delivery[54,57,58] or even cell encapsulation.[59] In order to employ polyglycerol as a multivalent selectin ligand, it can be easily sulfated with an SO_3/Pyridine complex under dry conditions as established by Turk et al.[60] The sulfation of polyglycerol has no noticeable effect on the cytotoxicity of the polymer.[61] dPGS with a degree of sulfation of 92% still exhibits exceptionally low cell toxicity and does not change cell numbers or cellular morphology as presented in the work of Haag and coworkers.[61] Due to the the importance of sulfates in selectin binding, dPGS proved to have an exceptionally high potential for targeting and treating inflammation.[60] Interestingly, dPGS exhibited much higher affinities than other tested polyanions.[62] Besides having an IC_{50} value for L- and P-selectin in the low nanomolar range,[63] dPGS has an effect on several proteins in the complementary system, which is one of the main reasons for its strong anti-inflammatory activity.[63] Furthermore, it could be shown by dye and radioactive labeling of dPGS that dPGS is rapidly internalized by hepatic Kupffer cells, HUVECs, and A549 cells.[61,64,65] As the cellular uptake of most polyanions is very limited,[61] this behavior is highly surprising and currently under investigation.[61] Most of these projects were performed with the same molecular weight dPGS of approximately 10 kDa.[62–65] Gröger et al. investigated the influence of size and degree of functionalization of the inhibition L-selectin:[21] By increasing the degree of sulfation from 10 to 83% on a 6 kDa PG core, a more than three orders of magnitude lower IC_{50} value was reported, as the higher degree of sulfation increased the multivalent enhancement.[21] Furthermore, it could be shown that IC_{50} values went from 100 nM to 23 pM upon increasing the dPGS size from 4 to 17 nm.[21] This is more than a three orders of magnitude increase in the inhibition potential by only a four-fold increase in diameter. This strong increase of inhibition potential was also assumed to be based on multivalent enhancement, but as the mechanism of globular binding inhibition remained unsolved (see Chapter 1.1.2), this could not be verified.[21] Nevertheless, in case the author's assumption is correct, comparing the multivalent enhancement on a 17 nm dPGS with the approximately 100 or > 1000 nm sized virus or leukocyte, respectively, the impact of multivalency on biological binding events could be enormous. For example, polymorphonuclear leukocytes have an average diameter of 3.75 µm and it could be calculated that the number of individual P-selectin/PSGL-1 interactions upon contact with the inflamed endothelium is as high as ~400/cell.[66] Hence, the number of multiple interactions might be much more important than the binding strength of a single ligand/receptor pair.[66] To study the

influence of the scaffold size on multivalency in detail, larger scaffolds are required. One approach would be the sulfation of PG-nanogels, a synthesis which has not been successful so far. My thesis involves the presentation of dPGS on gold nanostructures to enter size regimes that are comparable to biological binding events (Figure 1), and thus benefit from the multivalent enhancement as well as inherent properties of the nanomaterials for the preparation of an inflammation targeted contrast agent.

1.2.3 Polyanions and their application as viral entry inhibitors

Polyanions are known to have a two-way mechanism for the inhibition of viral infections. The first is a non-specific inhibition of the reverse transcriptase of various retroviruses,[67,68] but as polyanions are usually not internalized, this mechanism is only of minor practical relevance.[67,68] Therefore, this chapter focuses on the second inhibition mechanism, namely, the inhibition of the virus binding to cells by competition (see Chapter 1.1.2).

1.2.3.1 The binding of anions to viruses

In 1965 it was first postulated that polyanions interfere with the attachment of the virus to the cells.[69] In later research, it could be shown that polyanions only bind to envelope viruses like immunodeficiency virus (HIV), vesicular stomatitis virus (VSV), respiratory syncytial virus (RSV), and herpes simplex virus (HSV).[45,70,71] The binding inhibition of envelope viruses to cells by polyanions and especially polysulfates is not surprising, as it has been known for a long time that envelope viruses bind relatively unspecifically to the heparan sulfate on the glycocalyx of the host cells.[72] Envelope viruses contain a negatively charged lipid bilayer which would normally repel anions, but the inhibitory effect of polyanions appears to be based on their interaction with the protein layer surrounding the virus.[45] The concrete protein interaction differs for the various viruses and could in many instances not be specified, i.e., in the case of VSV.[73] In contrast, for HIV-1, polyanions are thought to bind to the V3 loop of gp120 and also the N-terminus of gp41.[74] This interaction appears to be relatively independent of the anionic group as its inhibition was observed for a large variety of polyanions like sulfated polysaccharides, negatively charged proteins, synthetic sulfated polymers, and even inorganic polyphosphates.[28,45] Nevertheless, sulfate and sulfonate terminated systems have been identified to have the highest inhibition potential,[35,75–77] while phosphonates are usually worse inhibitors for envelope viruses.[45,78] One very specific type of interaction which differs from the previous discussed general binding of polyanions is the binding of sialic acid (SA) to hemagglutinin (HA) and neuraminidase (NA) on the surface of influenza virus (see Chapter 1.1.2). Even though SA is basically anionic because of its carboxyl group, its binding to the hemagglutinin trimer of the viral surface is very specific and highly dependent on the type and sequence of the sugar

moieties.[79] However, as polyanions and SA functionalized inhibitors both act by the same concept of competitive binding inhibition, I will include SA based inhibitors in the discussion on polyanionic inhibitors.

1.2.3.2 Multivalent virus entry inhibitors

As discussed in Chapter 1.1.2, the multivalent presentation of ligands can significantly increase the binding affinity of inhibitors to viruses. Multivalent virus inhibitors can be divided into two classes. The first class are lower valent inhibitors with scaffolds which are optimized to present ligands at exact spacings to complement the binding pockets of a single receptor on the viral surface. A very nice example of this type of inhibitor was recently presented by the Meyer group who prepared a SA functionalized tripod with defined spacing for optimal binding to the HA trimer, which bound to HA5 with a dissociation constant of 446 nM.[33] The preparation of this kind of inhibitor is only possible if the structure of the receptor is perfectly resolved by X-ray or cryo-TEM, which is the case for the trimeric HA,[80–82] but not for every other receptor.

The second class of multivalent virus entry inhibitors are of much higher valency and are not optimized to the structure of a single receptor but are instead associated with larger scaffolds and the targeting of multiple receptors. My thesis will mainly focus on the preparation and evaluation of this type of inhibitor. For the inhibition of influenza virus by competitive binding inhibitors, a high variety of SA functionalized scaffolds have been reported in the literature (see Chapter 1.1.2). All of these SA functionalized scaffolds exhibited IC_{50} values orders of magnitude lower than for the monomeric SA unit, confirming the importance of the scaffold on the inhibition. So far, the largest virus inhibitors were SA functionalized dPGs and PG-nanogels that were prepared by the Haag group.[28] By simply increasing the size of the scaffold from 3 nm to 50 nm at a constant SA functionalization, the IC_{50} value for viral infection decreased from 153 μM to 8 nM.[28] Even though the spacing of SA was by no means optimized for the hemagglutinin structure, a simple 17-fold increase in scaffolds size resulted in a more than 4 orders of magnitude lower IC_{50} values. The high inhibition potential of the 50 nm SA functionalized PG-nanogel was encouraging because it proved that the presentation of ligands on virus-sized scaffolds could be highly beneficial. Nevertheless, up to the present, competitive binding inhibitors for other viruses, i.e., HIV and HSV,[70,71,83,84] are still based on inhibitor sizes < 10 nm. One example are gold nanoparticles ≤ 2 nm which were functionalized with monovalent, sulfated ligands.[70,71,85] Therefore, the polysulfated gold nanoparticles are much smaller than the 120 nm diameter of the virus itself.[86] Even though IC_{50} values for viral infection per ligand were already in the low micromolar range, virus-sized scaffolds could reasonably further enhance the inhibition potential. Especially for higher valent and larger inhibitors, the effect of steric shielding on the

competitive binding inhibition can be assumed to be significant. The exact influence of the scaffold size on the inhibition potential, however, can still not be predicted, even today, as the mechanism of competitive binding inhibition is still elusive (see Chapter 1.1.2).

1.2.3.3 Polyanionic virus inhibitors in vivo

Despite the previously shown effectiveness of polyanions *in vitro*, efforts to put polyanions as virus entry inhibitors to use in clinics have been unsuccessful. In 1989, dextran sulfate was tested as an anti-HIV agent in a clinical trial by oral administration but did not perform any better than the control group.[87] This result was not really surprising, as simultaneously it was shown that the oral administration of the drug resulted in poor uptake into the blood.[88] Two years later, the drug was *i.v.* administered to 10 HIV infected patients for 14 days at a 200-fold dose higher than the IC_{50} value for HIV infectivity *in vitro*.[89] Despite the high dose, the HIV p24 antigen levels significantly increased in all subjects who received the drug for more than three days.[89] After these initial letdowns, clinical trials of polyanions as antiviral agent have been restricted to topical application for the prevention of infection. Currently, the most advanced system is Vivagel® (SPL7013), which is a G4 poly-L-lysine based dendrimer peripherally functionalized with a total of 32 sulfonate groups and an approximate hydrodynamic diameter of 5 nm.[90] Even though *in vitro* studies have provided encouraging evidence for the antiviral activity of Vivagel® against HIV and HSV,[83] it did not reach the market for *in vivo* application due to limited efficacy in clinical trials.[83,91,92] In summary, despite promising *in vitro* results for the treatment and prevention of enveloped virus based infections by polyanions, the high hopes could not be retained *in vivo*. Especially in comparison to the other approximately 30 drugs which are currently approved in the United States for treatment of HIV,[93] competitive virus-binding inhibitors based on polysulfates are still inferior. For example, one very successful upcoming antiviral agent is Tenovir®, a reverse transcriptase inhibitor which was able to reduce the number of HIV incidences of 2413 participants by up to 74% in a recent clinical trial 2013.[94] To evaluate if competitive binding inhibitors have a long-term chance to compete with other state-of-the-art antiviral agents, inhibitors have to be optimized to their best potential, which requires a detailed understanding of the inhibition mechanism. Since the high inhibition potential of the virus sized inhibitors prepared by Bathia et al. has been encouraging, this thesis will now focus on the evaluation of virus-sized inhibitors based on dPGS functionalized gold nanoparticles.

1.3 Inorganic nanomaterials for biomedical applications

For the preparation of dPGS functionalized colloids which are suitable for theoretical investigations on multivalency and for biomedical applications, the requirements for synthesis and properties have to be understood. This section will give a brief overview of the preparation, properties, and application of inorganic nanomaterials with a special focus on polysulfated nanostructures.

1.3.1 Stability of colloidal dispersions – The DLVO theory

One of the most important properties of colloids is the very high surface area to mass ratio due to the small dimension of the particles. Thermodynamically, a large surface area is energetically unfavorable, thus, in order to avoid aggregation, the particles have to be stabilized. In the 1940s, a major breakthrough in colloidal science occurred due to the establishment of a theory that quantitatively described the energy-distance curves of charged nanoparticles.[95,96] The DLVO (Derjaquin-Landau-Verwey-Overbeek) theory assumes that the nanoparticle stability is mainly governed by the interplay of long ranged Van der Waals attraction and electrostatic double layer repulsion (Figure 5).[96]

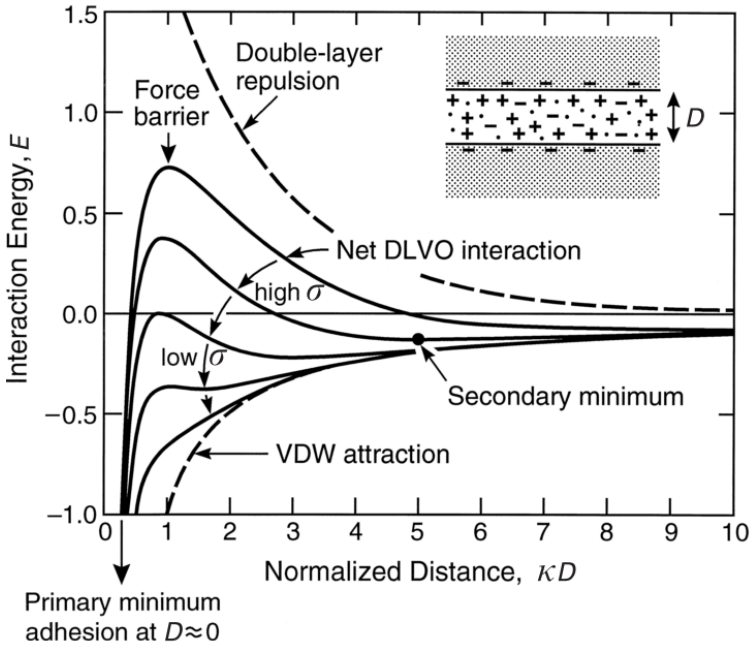

Figure 5. Schematic presentation of the total interaction energy *E* between two negatively charged particles in a aqueous electrolyte solution dependent on the surface charge density σ, the distance between the particles *D* and the Debye-Hückel parameter κ. Reproduced with permission from Leite et al.[96] Copyright 2012 MDPI.

From the DLVO theory, the repulsion and attraction of particles is dependent on the total electrostatic repulsion and the Van der Waals attraction, respectively. The subtleties in the plots are due to the distance dependencies of the electrostatic repulsion and the VdW attraction, with the first being exponential and the second a power law.[97] If the force barrier (Figure 5, continuous line) is negative, particles will spontaneously aggregate. If it is positive, in dependence on the interparticle distance *D* and the Debye-Hückel parameter κ the particles will be in the primary minimum or the secondary minimum.[97] The primary minimum describes the state of irreversible aggregation, which can occur at high temperatures, high ionic strengths or under the application of strong external forces like centrifugation. The secondary minimum describes attractions which are usually not strong enough to result in adhesion; however, larger particles can form flocculates, which are strong enough to resist brownian motion but may dissociate under an externally applied force such as vigorous agitation.[97] In practice, the colloidal stability can be tuned by several means. The pH of the solution dictates the protonation state of the ionic groups on the particle and, therefore, the surface charge density σ.[96] Polysulfated nanoparticles are much less influenced by changes in the pH of the solution, as sulfate groups are not protonated under conditions which are relevant for experiments and applications.[98] As a result, polysulfates are especially good for stabilizing nanomaterials. Furthermore, a high ionic strength of a medium results in a compression of the electric double layer and therefore, the Debye length, which is the inverse of the Debye-Hückel parameter κ.[96,97] As a result, higher ionic strength solutions increase the chance of particle aggregation. This is a major problem for the *in vivo* application of nanoparticles, in which case the ionic strength is usually around 150 mM.[38] In order to circumvent this problem, colloids can be sterically stabilized by coating them with bulky ligands like polymers. When the stabilizing moieties of two converging particles overlap, the osmotic pressure inside this layer increases and the particles are pushed apart.[99] The interparticle distance is thus outside of the primary minimum and the particles are stabilized. Theoretically, this makes the polyanion dPGS a very suitable ligand for the stabilization of nanomaterials as it stabilizes the colloids sterically and electrostatically. This type of stabilization is termed electrosteric stabilization.[99] It is important to remember that the DLVO theory is a very simplistic view of the interparticular interaction of nanoparticles, even though it is very effective in many cases. Since important factors like multivalent counterions, depletion, hydrogen bonding, hydrophobic and entropic effects are disregarded in this theory,[100] it can only be applied in specific cases. Especially when immerged in biological media the reality turns out to be much more complex, as the nanoparticles are immediately covered in a protein corona.[38] The interactions present at the nano-bio interface are briefly discussed in the next section.

1.3.2 Biocompatibility of colloids

Especially under physiological conditions, nanoparticles are subjected to harsh conditions like high temperature, high ionic strength, oxidative/reductive conditions, and a large variety of biomolecules.[38] The impact of these conditions on the stability and biocompatibility of colloids are summarized in an excellent recent review by Nel et al.[38] Briefly, the interactions of colloids with biological components are highly dependent on the coating of the nanoparticle, the core material, and the size and shape of the colloid. Furthermore, the coating of the nanoparticle mainly governs the formation of the protein corona covering the nanoparticular surface, a process also known as "opsonization".[38,101] The formation can be based on charge interactions, hydrophobic interactions, or interactions of functional ligands that have been immobilized on the nanoparticle with specific proteins in the medium. The general biocompatibility of colloids depending on their core size as well as surface functionalization is depicted below (Figure 6).

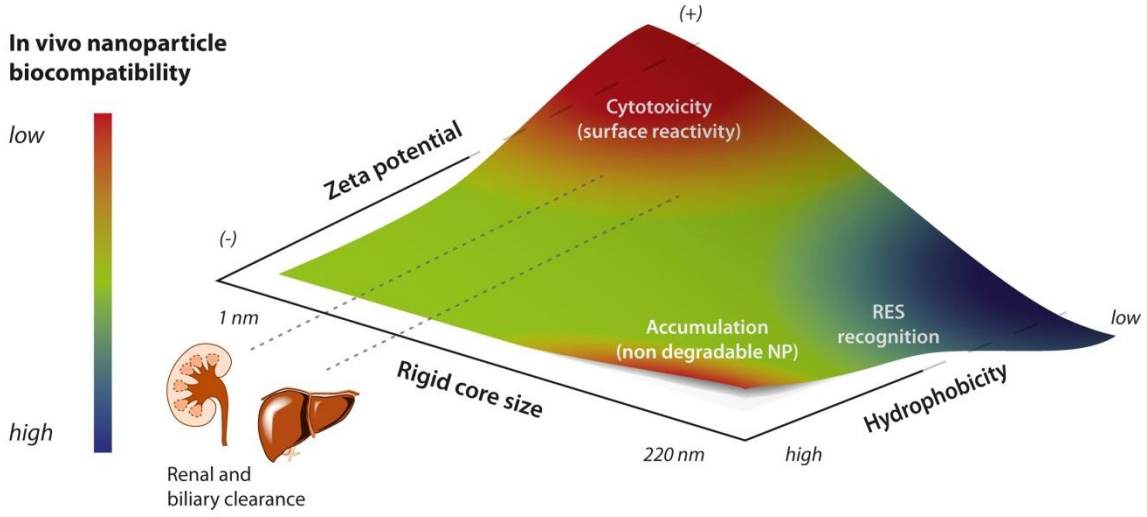

Figure 6. Qualitative description of colloid biocompatibility after *i.v.* administration, based on the evaluation of more than one hundred nanoparticles.[38] Reproduced with permission from Nel et al. Copyright 2009 Nature Publishing group.

There is a general trend for the biocompatibility of colloids. Smaller sized anionic colloids with hydrodynamic diameter below 6 nm are generally highly biocompatible. Because of the anionic charge, their toxicity is limited, whereby the small particle size permits renal clearance.[38] Cationically charged colloids are the most cytotoxic, as their positive charge leads to lysis of the cell membranes and platelet aggregation.[38] A similar trend is observable for larger colloids with several tenths to hundreds of nanometers. Even though anionic colloids of this size still exhibit very low cytotoxicity,[38] their application *in vivo* is limited. Particles of this diameter cannot be cleared by the kidney anymore but strongly accumulate in organs associated with the reticuloendothelial system

(RES).[38][101] The recognition of particles >200 nm by macrophages happens regardless of charge, and significantly reduced plasma half-lifes in the blood are observed. Nevertheless, the adsorption of proteins on nanomaterials further accelerates their elimination by the RES.[101,102] Hence, higher particle concentrations or multiple injections are required for *in vivo* applications of ionic nanoparticles. As a result, the toxicity of the core material is of major importance. Especially inorganic cores can have a number of toxic effects depending on their material. ZnO, Ag, Co/Ni, Cu and CdSe can all release toxic ions.[38] Many of these surfaces furthermore enhance the reactive oxygen species (ROS) production and induce inflammation. Gold still counts as the most non-toxic core material for nanoparticles, as its only toxic effect is based on the deformation of proteins upon hydrophobic adsorption. This effect can be easily suppressed by functionalizing the nanoparticles with a protein resistant layer. Nevertheless, it is important to remember that even the strongest nanoparticle coating can only resist harsh physiological conditions a limited period of time. If the nanoparticles are not excreted, the core material of any nanoparticle will be exposed to the body sooner or later, even if not within the period of observation. Iron oxide based nanoparticles have a significant advantage, as the iron can be absorbed by the body after dissolution of the core and integrated into the physiological iron storage.[103,104] Another important factor which dictates the interaction of colloids with biological surfaces is their shape. Anisotropic shapes of larger sized colloids generally result in higher cytotoxicity, as observed for carbon nanotubes. The phagocytes literally impale themselves when trying to engulf the nanotubes, a process commonly known as frustrated phagocytosis.[105] The cellular uptake of gold nanorods that were 14 nm x 74 nm also significantly differed from that of either 14 nm or 74 nm gold nanospheres,[106] also indicating a dependence on the aspect ratio. In this case, the exact uptake mechanism is still unknown.

Part of my thesis will include the functionalization of gold colloids with dPGS. The highly anionic polymer layer will facilitate the stabilization of the colloid under physiological conditions as well as provide an acceptable biocompatibility. Nevertheless, due to the lack of excretion pathways, these structures are only partially suitable for *in vivo* applications.

1.3.3 Synthesis of inorganic nanoparticles

Chemists usually employ a bottom-up approach for the preparation of inorganic nanoparticles. The formation of nanoparticles is generally achieved by increasing the concentration of the core forming solute above the critical nucleation concentration (C_{nuc}) as commonly described by the LaMer diagram (Figure 7).[107]

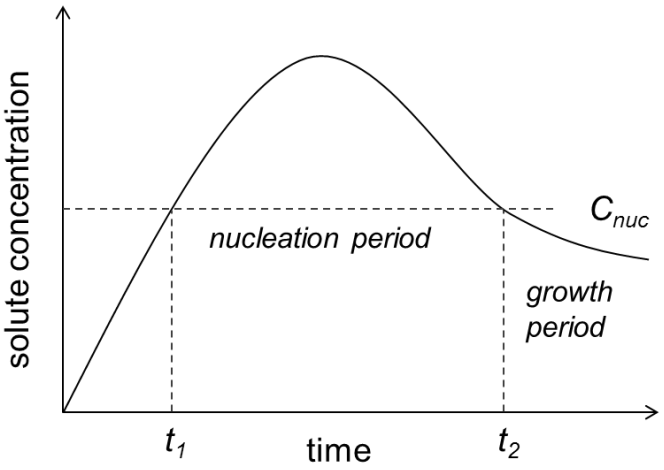

Figure 7. Concentration of dissolved solute before (t_1) and after (t_2) the nucleation period as a function of time.[107] When the concentration of the dissolved solute exceeds the nucleation concentration (C_{nuc}), nucleation takes place.

When the solute concentration reaches the nucleation concentration C_{nuc}, inorganic nanoparticles are formed. As a result, the concentration of the solute decreases until it falls below C_{nuc}. At this stage, no further nucleation takes place and additional solute fully contributes to the growth of the already existing nanoparticles.[107] The solute should be formed in a continuous manner, as this permits the regulation of the nucleation period according to the rate of solute formation. The different mechanisms for solute formation can vary significantly depending on the metal employed. Most common mechanisms are based on the continuous formation of a zero valent metal from a metal precursors, either by reductive, thermal, microwave assisted, or hydrolytic means.[108] More recent protocols for the formation of metal nanoparticles or nanosheets also employ a local restriction of the solute concentration using microemulsions or liquid-liquid interphases, respectively.[108] The formation of gold colloids, as employed in thesis, is mainly performed by chemically reducing a metal precursor to the elementary gold. The most popular route for the synthesis of gold nanoparticles was reported by Hauser and Lynn.[109] The procedure involves the reduction of chloroauric acid in a boiling solution of sodium citrate, whereby the citrate acts equally as a reducing and stabilizing agent. By varying the initial citrate concentration, different rates of reduction and, as a result, longer or shorter nucleation periods can be achieved. By this procedure, gold nanoparticle of 10 nm to 100 nm can be prepared.[110,111] Nevertheless, the quality of the larger sized particles obtained by this procedure is quite poor, as parallel nucleation processes are often observed and the resulting particles are ill-shaped. Recently, Li et al. and Ziegler et al. independently established protocols to circumvent this problem by a seed growth mechanism.[112,113] Li et al. regulated the reduction of the chloroauric acid by the addition of hydroquinone, which has a high selectivity in reducing Au^I to Au^0 on the gold seed

surface and suppresses additional nucleation. The resulting particles take on an urchin-like morphology, which can be later reformed into a spherical shape by thermal means. In contrast, the procedure established by Ziegler et al. for the synthesis of larger gold nanoparticles, is based on the separate, continuous addition of sodium citrate, ascorbic acid and chloroauric acid to a seed dispersion of smaller sized gold nanoparticles.[113] As presented in the LaMer diagram (Figure 7), the slow addition of the reagents results in a solute concentration below the critical nucleation concentration so that all the particles grow without additional nucleation. This procedure results in a monomodal size distribution with very low polydispersity and is currently the state of the art for the synthesis of larger gold nanoparticles and was employed in the experimental work of this thesis.

1.3.4 Stabilizing ligands and functionalization of inorganic nanoparticles

One very important aspect about the synthesis of inorganic nanoparticles is the type of the stabilizing agent which coats the nanoparticles after synthesis. Both of the most common synthetic procedures for the preparation of AuNP < 10 nm result in particles stabilized with alkane-thiols after synthesis.[114,115] Even though the synthesis is well controlled, the ligand exchange reaction of the alkane-thiols with hydrophilic ligands can be very problematic. Another extreme example for problematic stabilizing agents after the synthesis of colloids is cetyltrimethylammonium bromide (CTAB). This cationic surfactant is widely applied for the synthesis of inorganic colloids as is has two critical micelle concentrations (CMC),[116,117] of which the higher CMC results in the formation of rod-like micelles. These rod-like micelles can be employed as template for the preparation of anisotropic colloids, i.e., gold nanorods,[116,118] in which case the cationic head group coordinates to the facets of the gold surfaces with different affinities and induces a breakage of the symmetry.[118] Gold nanorods are very interesting for biomedical application because of their large contact area with biological surfaces and absorption of light in the near infrared region (Chapter 1.3.5). Nevertheless, the requirement of CTAB for the synthesis of gold nanorods significantly complicates their biomedical application as CTAB is highly toxic because of its ability to disrupts the cell membranes.[119] With the high concentration of CTAB required for the formation of rod-like micelles (~250 mM),[120] the synthetic reaction mixture is a toxic bomb. Removal of free CTAB by centrifugation is not possible as a critical [CTAB]/[AuNR] ratio of $7.4 \cdot 10^5$ is required for the stabilization of colloid.[121] Several protocols for the passivation have been established, of which most are based on the ligand exchange of CTAB with thiolated PEG.[122–124] The functionalization of cationically stabilized colloids with anionic ligands is particularly challenging. Simple ligand exchange reactions are not possible because of the strong electrostatic attraction of the ligands, which usually results in aggregation of the colloids. One possible solution is the layer-by-layer functionalization of the CTAB-stabilized gold nanorods with several layers of linear polyanions and polycations.[125–127] Even though the authors claim that the resulting

nanorods are stable under physiological conditions, the stability of the polyelectrolyte layers at an 150 mM ionic strength is questionable and none of these colloids ever made it to *in vivo* experiments. Furthermore, significantly amounts of CTAB are still adsorbed on the nanorod surface as within the polyelectrolyte layer, which results in significant residual cytotoxicity.[119,128–131] Alternatives are the coating of the nanorods by a silica layer before functionalization, or a round-trip phase transfer of the gold nanorods,[124,132] both of them having significant disadvantages. The coating of gold nanorods in a silica layer often results in irreversible aggregation of the colloids as the layer itself is poorly stabilized during growth. This is best observed by the presented TEM micrographs of the formed nanorods, as no individual particles are present but they are all connected by small "silica bridges".[124,133] Furthermore, the growth of the silica layer is not directional, thus larger layer thicknesses result in a more spherical form of the coated nanorods. Therefore, they lose their characteristic cylindrical surface which permits large contact areas with biological surfaces. The third method, namely the round-trip phase transfer, requires the protonation/deprotonation of mercaptocarboxylic acids. As a result, this procedure is only applicable for the preparation of carboxyl functionalized nanorods. Summing up, there is currently no convenient method present for the preparation of anionic functionalized gold nanorods of low toxicity.

The type of anchor group for the connection of the ligand with the inorganic surface is another very important aspect to keep in mind while functionalizing inorganic colloids. For synthesis, usually weaker binding anchor moieties are favored, as they facilitate ligand exchange reactions with stronger binding, functional ligands.[134] For application, stronger binding anchor moieties are usually required, due to the enhanced stability of the formed colloids and higher ligand densities on the nanoparticular surface.[134] Anchor moieties generally inherit an electron donating group such as thiol,[135,136] amine,[137] carboxyl or phosphine.[134] The thiol group has the strongest coordination to most of the metals employed for inorganic nanoparticles, especially to gold were the binding energy is approximately 200 kJ/mol.[135] Nevertheless, it is important to remember that even the thiolated ligands can undergo dynamic binding and unbinding processes.[138] In order to increase the long-term stability of gold colloids stabilized with thiolated ligands, many scientists employ a multivalent presentation of thiol groups to enhance the stability.[56,136,139–143] For gold nanoparticles, the use of disulfide anchor moieties is often sufficient,[142,143] thus the most commonly employed anchor group is nowadays thioctic acid.[56,136,139–142] For semiconducting nanoparticles, which exhibit weaker binding to thiols, Mattoussi and coworkers have taken this approach to the next level and functionalized quantum dots with multivalently presented thioctic acid moieties.[139,144,145] The resulting particles were stable even after a year of storage under high temperature and high ionic strength. One part of my thesis will focus on the preparation of polysulfated gold nanorods with low cytotoxicity by the establishment of new procedure for the anionic functionalization of gold nanorods. For this, I will use the enhanced binding strength of disulfides in comparison to monovalent thiol anchors.

1.3.5 Material-derived properties and applications of inorganic nanomaterials

Inorganic colloids have certain properties which are otherwise hard to achieve by polymeric approaches. Generally, they are very dense and are mostly constituted of high atomic mass elements, which results in a high signal, or contrast, in any photon or electron based characterization techniques like TEM,[17] DLS,[146] DIC,[147] or SPR.[148] Furthermore, when decorated with functional ligands, the high density of the core permits the purification of particle bound biomolecules simply by centrifugation. One very advantageous property of all inorganic colloids, which is often underestimated, is the possibility to determine the concentration of metals with high sensitivity and accuracy via AAS or ICP-MS.[149] This is especially advantageous for *in vivo* applications, as the physiological amount of most metals is very low and, therefore, permits a good signal-to-noise ratio.[149] The material of the core also highly influences their physical properties. For example, iron oxide based colloids are superparamagnetic in dependence on their size.[104] In simple words, this means they are only magnetic when an external magnetic field is applied. Their specific properties permits a vast range of applications like magnetic removal of biomolecules from complex biological mixtures, magnetic immunoassays (MIA), magnetically targeted drug delivery, magnetic hyperthermia or *in vivo* imaging via magnetic resonance imaging.[104] The possibility of these particles to combine therapy and diagnostics in one compound opened-up the new and extremely fast growing field of so-called "theranostics".[150] Another important size-dependent physical property includes the quantum confinement effect of nanoparticles which are based on semiconducting materials like InGaAs, CdSe or GaInP/InP.[151] These kinds of particles are commonly known as quantum dots and are because of their fluorescent properties with high quantum yields, superior photothermal stability and size-dependent emission/excitation wavelength widely applied in the field of life sciences.[152] In contrast to semi-conducting cores, if light is shone on nanoparticles of conducting metals, i.e., silver or gold, the electrons within the core will resonate and absorb energy of a certain wavelength. The wavelength of the adsorbed light is dependent on the dimension of the colloid and will increase with larger particle sizes.[153] For gold nanoparticles of ≤ 30 nm, this adsorption lies at the blue-green range of the visible spectrum of approximately 500 nm, resulting in the characteristic red color of gold nanoparticle dispersions.[153] The extinction coefficient as well as adsorption maxima of gold nanoparticles in dependence on their size can be exactly described by the Mie theory,[154] which enables the direct quantification and size determination of the nanoparticles simply by UV-Vis measurements.[153] Even easier, as the adsorption wavelength of gold nanoparticles is within the visible spectrum of light, aggregation phenomena can be identified simply by the eye. This is a massive advantage of conducting nanoparticles over non-conducting particles, and makes them perfectly suitable for model investigations. Anisotropic gold colloids on the other hand have several surface plasmon resonances in dependence on their geometry.[154] Electrons within a gold nanorod for example have a longitudinal resonance and a transversal resonance with adsorption maxima at approximately 500 and 800 nm,

respectively.[155] The near-infrared, longitudinal absorption maximum is hereby especially relevant for biomedical applications as it is place directly within the lowest adsorbing wavelength range of water and hemoglobin with 650-900 nm.[156] This property can be used for the excitation of the nanorods by high energetic lasers and as gold nanorods have one of the highest photothermal conversions known in literature,[157] a vast amount of the energy is transformed into heat. Hence, a continuous excitation will result in a significant temperature rise of the surrounding tissue, which in combination with the EPR effect (see Chapter 1.3.6) enables the photothermal therapy of cancer.[158] Alternatively, if the nanorods are excited in a pulse-wise manner they will alternatingly expand and contract. The acoustic waves which are emitted by this process can be detected and the localization of the nanorods determined. This process is commonly known as optoacoustic imaging and has significant advantages over optical imaging as the emitted waves are not affected by tissue scattering.[159] The most modern technique based on this technology is multispectral optoacoustic tomography (MSOT),[157] which permits *in vivo* imaging with a spatial resolution comparable to MRI or XrayCT, but at significantly lower cost.[157] Even though the multiple and long wavelength adsorption properties of gold nanorods makes them theoretically more useful for optical based biomedical application than gold nanospheres, their *in vivo* use is still limited due to the requirement of CTAB for synthesis (see Chapter 1.3.3). Furthermore, it is still not possible to quantitatively relate the UV-VIS absorption profile of AuNRs to the geometry and concentration, which significantly complicates their characterization in contrast to nanospheres. For applications which do not require absorption in the near-IR region, gold nanospheres are because of their ease of synthesis, functionalization and characterization still the scaffold of choice.

1.3.6 Dimension-derived properties and applications of inorganic nanomaterials

Besides the functionalization of nanomaterials with biologically active ligands, the dimension of colloids is another property which can be influenced to control their biological interaction behavior by physical means. Limited by their size, colloids can under normal circumstances not penetrate endothelial tissue by intercellular pathways.[160] In contrast, the highly accelerated growth of tumorous tissue results in vast intracellular gaps of up to 400 nm, which permits the penetration of nanoparticles. Therefore, the colloids specifically accumulate in the cancerous tissue. This effect is commonly known as enhanced permeation and retention (EPR),[160] and has since its discovery in the 1986 by Maeda and Matsumura become the gold standard for targeted tumor diagnosis and therapy.[19,130,161–168] Furthermore, the dimension of the nanoparticle strongly dictates the contact area with other surfaces and, as a result, multivalent effects. Nanomaterials are usually multifunctional by nature and their mild, facile, and chemoselective functionalization permits the presentation of a wide variety of ligands. The number of multiple interactions which results from the multivalent presentation of ligands on nanosized materials is often several orders of magnitude higher than in the case of polymeric

examples.[17,28,169] As discussed in Chapter 1.1, the multivalent binding constant increases with the number of multiple ligand/receptor interactions by a power law,[5] which results in binding constants of such high magnitudes that they are unusual for most chemists or biologists. This is even more pronounced when the shape of colloids is optimized for large contact area and, therefore, number of interactions with its partner. One very nice example on the importance of the nanoparticle shape and thus contact area, is a comparison of the binding constants between oligonucleotide functionalized gold nanospheres, nanoprisms and nanorods. By simply changing the shape of gold nanostructures from spheres to prisms at normalized number of ligands, the affinity after hybridization of the complementary particles was several million times higher for the nanoprisms than for the nanospheres.[170] The multivalent nature of gold nanoparticles and the possibility to precisely adjust their size and shape by current synthetic procedures (see Chapter 1.3.3), make nanoparticles especially suitable for self-assembly processes as in the field of DNA origami or nanoparticle supracrystals. The Mirkin group functionalized gold nanoparticles with complementary DNA strands for the formation of nanoparticle based superlattices.[171] The binding of the resulting particles by hybridization could be reversibly controlled by the applied temperature. The thermally induced reorganization of the particles resulted in the growth of nanoparticular lattices with characteristic crystallographic symmetries and lattice parameters, which were strongly dependent on the employed particles sizes. Finally, the results could even be related to the structure of ionic crystals and resulted in the definition of fundamental rules for the preparation of superlattices.[171] The establishment of fundamental rules of this kind is only possible with a highly controlled system which is can be precisely characterized, as given by the high contrast of gold nanoparticles in TEM and SAXS measurements. The same beneficial properties of gold nanoparticles were employed by the Grzybowski group for the formation of nanoparticle supracrystals.[172] In this new field, gold nanoparticles of various sizes are respectively functionalized with polyanionic and polycationic ligands. The highly charged and well defined particles have similar properties to ions only on a nano-scale and are therefore called “nano-ions”.[173] Those nano-ions spontaneously assemble into nanoparticle supracrystals of up to micrometer sizes and have in combination with their physical properties a wide variety of possible applications in the field of opto-electronics,[174] high-density data storage,[175] catalysis,[176] and biological sensing.[177] More recently, gold supracrystals could also be employed for the preparation of a new type of material, which has the same conducting properties as metals but a plastic-like rheology.[178] This fascinating material can be processed by techniques commonly employed in the polymer industry, but hardens at 50 °C to form the bulk metal.[179] In summary, the possibility to precisely tune the size of gold nanoparticles in combination with the easy functionalization by thiolaled ligands and good characterizability, make gold nanoparticles perfectly suited for the investigation of size-dependent effects. As the possible dimensions of gold nanoparticles overlap with the size of many viruses (Figure 1), my aim in this thesis is to employ their beneficial properties to establish a model describing the binding inhibition of viruses by multivalent inhibitors.

2. Motivation and Objective

It is well known that polysulfates actively target inflamed endothelium and various envelope viruses. While dendritic polyglycerolsulfate (dPGS) has already emerged as highly potent candidate for the targeting and treatment of inflammatory diseases, it should also be investigated for its potential as virus entry inhibitor. As the targeting properties of dPGS are based on multivalent binding, increasing the size of it to virus-like dimensions should significantly enhance its binding properties due to larger contact areas with viruses and the inflamed endothelium, respectively.

In order to benefit on multivalent effects for the imaging of inflammatory diseases, gold nanorods should be functionalized with dPGS. Because of their very large contact area with the inflamed endothelium, dPGS functionalized nanorods could be very effective for targeting purposes. Furthermore, due to the inherent near-IR absorption of the anisotropic gold core, they could either serve as contrast agent for photoacoustic imaging or as photon absorber for photothermal therapy. Besides, a novel procedure for the functionalization of CTAB coated gold nanorods with polyanionic ligands, which on the one hand decreases the toxicity of the gold nanorods, and on the other hand, results in well dispersed nanorods which are stable even under physiological conditions, is urgently required.

For the inhibition of viral infections, dPGS functionalized gold nanoparticles of various sizes should be prepared. The combination of high binding affinities of with strong steric shielding effects could potentially result in highly potent virus entry inhibitors. Furthermore, an elucidation of the mechanisms involved in the competitive binding inhibition of multivalent targets with multivalent inhibitors is desperately needed, as this could permit the establishment of principles for the rational design of efficient viral inhibitors. Nevertheless, this requires the quantification of the size-dependent steric shielding effect.

Therefore, the main objectives of my thesis are (1) establishing a new procedure for the preparation of dPGS functionalized gold nanorods as contrast agent for imaging inflammatory diseases and (2) preparing polysulfated gold nanoparticles for the inhibition of viral infections and using them as model system in order to elucidate the mechanism of competitive binding inhibition.

3. Publications and Manuscripts

In this chapter the published articles as well as submitted manuscripts are listed and the contributions of the author are specified.

3.1 Polyglycerolsulfate functionalized gold nanorods as optoacoustic signal nanoamplifiers for *in vivo* bioimaging of rheumatoid arthritis

Jonathan Vonnemann,* Nicolas Beziere,* Christoph Böttcher, Sebastian B. Riese, Christian Kuehne, Jens Dernedde, Kai Licha, Claudio von Schacky, Yvonne Kosanke, Melanie Kimm, Reinhard Meier, Vasilis Ntziachristos and Rainer Haag

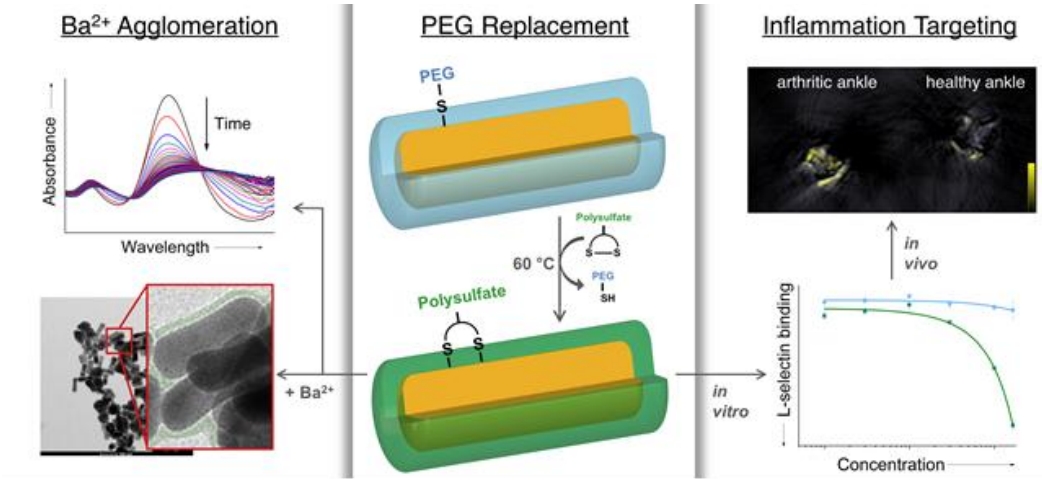

Figure 8. Adapted with permission from Vonnemann et al.[180] Copyright 2014 Ivyspring.

In this publication the author contributed with parts of the concept, the synthesis and characterization of the dPGS functionalized gold nanorods and the preparation of the manuscript.

Vonnemann, J.; Beziere, N.; Böttcher, C.; Riese, S. B.; Kuehne, C.; Dernedde, J.; Licha, K.; Schacky, C. von; Kosanke, Y.; Kimm, M.; et al. Polyglycerolsulfate Functionalized Gold Nanorods as Optoacoustic Signal Nanoamplifiers for *in vivo* Bioimaging of Rheumatoid Arthritis. *Theranostics* **2014**, 4, 629–641.

http://dx.doi.org/10.7150/thno.8518

3.2 Virus inhibition induced by polyvalent nanoparticles of different sizes

Jonathan Vonnemann, Christian Sieben, Christopher Wolff, Kai Ludwig, Christoph Böttcher,* Andreas Herrmann* and Rainer Haag*

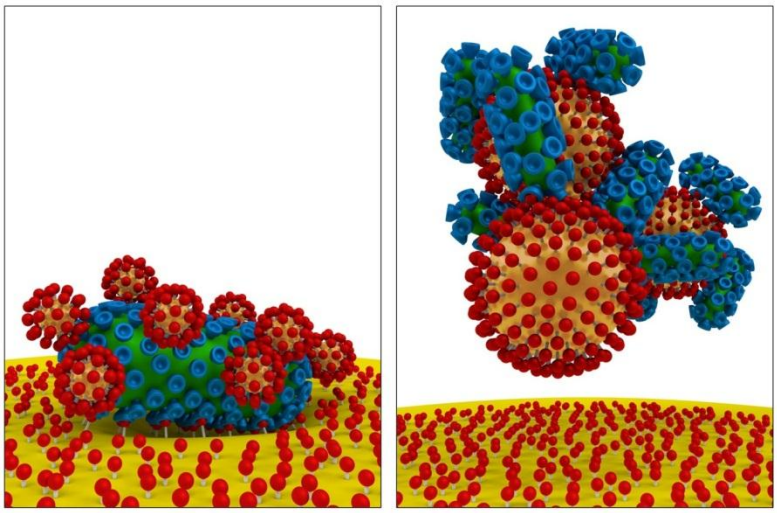

Figure 9. Reproduced with permission from Vonnemann et al.[181] Copyright 2014 Royal Chemical Society.

In this publication the author contributed with parts of the concept, the synthesis and characterization of the PGS-dendron functionalized gold nanoparticles and the preparation of the manuscript.

Vonnemann, J.; Sieben, C.; Wolff, C.; Ludwig, K.; Böttcher, C.; Herrmann, A.; Haag, R. Virus Inhibition Induced by Polyvalent Nanoparticles of Different Sizes. *Nanoscale* **2014**, *6*, 2353–2360.

http://dx.doi.org/10.1039/C3NR04449A

3.3 Size Dependence of Steric Shielding and Multivalency Effects for Globular Binding Inhibitors

Jonathan Vonnemann,* Susanne Liese,* Christian Kuehne, Kai Ludwig, Jens Dernedde, Christoph Böttcher, Rainer Haag and Roland R. Netz

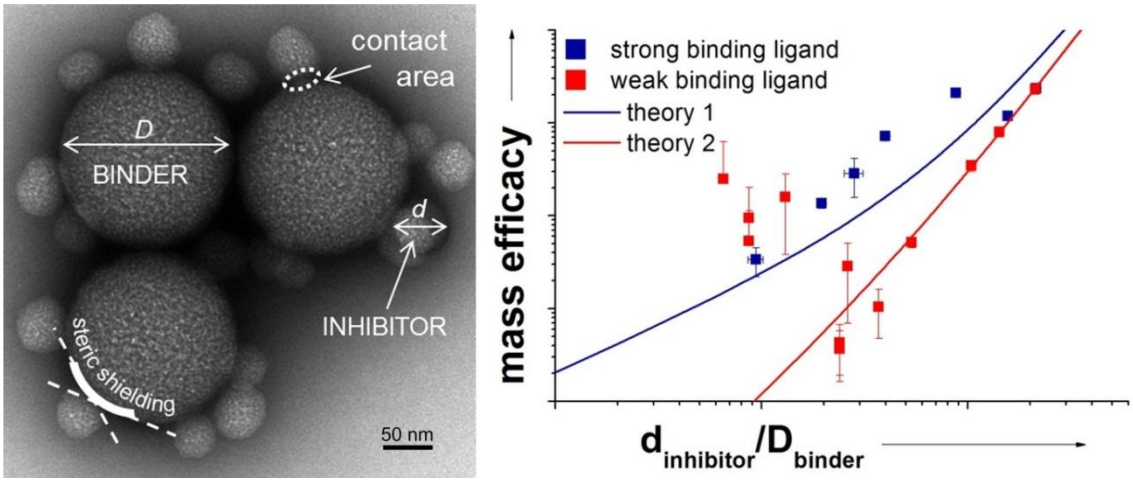

Figure 10. Used with permission from Vonnemann et al.

In this publication the author contributed with the concept, the synthesis and characterization of the nanoparticles, establishment the biotin/streptavidin inhibition assay, parts of the SPR measurements and the preparation of the manuscript.

Vonnemann, J.; Liese, S.; Kuehne, C.; Ludwig, K.; Dernedde, J.; Böttcher, C.; Netz, R. R.; Haag, R. Size Dependence of Steric Shielding and Multivalency Effects for Globular Binding Inhibitors. *J. Am. Chem. Soc.* **2015** in press, DOI: 10.1021/ja5114084

http://dx.doi.org/10.1021/ja5114084

4. Summary and Conclusion

Based on the knowledge that polysulfates bind to L-selectin and envelope viruses with high affinity, gold colloids were functionalized with dPGS and PGS-dendrons and were evaluated for their inflammation targeting and viral infection inhibition properties, respectively.

The first part of my thesis was focused on the synthesis of dPGS functionalized gold nanorods to benefit on their large contact area with biological surfaces and their inherent near-infrared absorption for the preparation of a contrast agent for the *in vivo* bioimaging of rheumatoid arthritis via multispectral optoacoustic tomography.[180] The major challenge in this project was the anionic functionalization of the initial CTAB-stabilized gold nanorods. Already established protocols in literature were disadvantageous as previously discussed in detail (see Chapter 1.3.4). Briefly, the resulting gold nanorods by these procedures either incorporate significant amounts of adsorbed, highly toxic CTAB or were only applicable for carboxylic acids. Hence, a novel protocol for the functionalization of CTAB-stabilized gold nanorods with polyanions based on a two-step ligand exchange reaction was established. In this procedure, the CTAB layer was first exchanged against a low molecular PEG-thiol, which after purification of the nanorods was further replaced by a high molecular thioctic acid (TA) functionalized dGPS at elevated temperatures. The reaction was entropically favored as the low molecular weight PEG_{1000} was exchanged against the much larger dPGS 10 kDa, as well as enthalpically favored due to the bivalent thioctic acid anchor group on the dPGS. The resulting dPGS functionalized gold nanorods (AuNR-dPGS) showed significantly lower cytotoxicity than other polysulfated gold nanorods from literature,[129] possibly due to the complete removal of CTAB before the anionic functionalization. The inflammation targeting potential of the AuNR-dPGS was investigated *in vitro* by competitive binding inhibition assays with leucocytes and L-selectin functionalized gold nanoparticles, respectively, for which in both cases AuNR-dPGS exhibited a very high binding affinity to the binder. In this project, the importance of a thorough purification after the functionalization of inorganic nanoparticles with polymers became clear. Because of the already very low IC_{50} value of dPGS itself, even vanishingly low amounts of free ligand resulted in absurdly low IC_{50} values for the AuNR-dPGS. As the scattering of the inorganic gold core in DLS and zeta potential measurements is orders of magnitude larger than for dPGS, these impurities were “hidden” in the respective measurements. Therefore, a simple test to prove the absence of dPGS by employing the inherent UV-Vis adsorption of the gold nanorods was established. When gold nanorods aggregate, their close proximity results in plasmon-plasmon coupling and, as a result, changes their UV-Vis absorption spectra and visible color. This phenomenon could be observed when a solution of $BaCl_2$ was added to a highly pure AuNR-dPGS solution, in which case the bivalent Ba^{2+} induced aggregation. For impure AuNR-dPGS solutions with unbound ligands, no color change

could be observed, as the aggregated AuNR-dPGS were too far apart for plasmon-plasmon coupling because of the additional layer of unbound dPGS in between the nanorods. This simple, macroscopic test proved to be of great value for the preparation of dPGS functionalized colloids. The inflammation targeting properties of AuNR-dPGS could also be reproduced in an animal model of rheumatoid arthritis. While PEG functionalized gold nanorods did not show an increased signal for the inflamed leg in MSOT imaging, the signal of AuNR-dPGS was 1.7 times higher in the inflamed leg than in the healthy leg. This was the first example of actively targeted gold nanorods in literature, and proved the feasibility of the multivalent presentation of low affinity ligands as a concept for targeting of gold nanorods. Nevertheless, even though the AuNR-dPGS very strongly retained in the inflamed tissue, they also had a much lower half-life in the blood than AuNR-PEG. This is probably based on the known opsonization[38,101] of charged colloids and, therefore, faster uptake by macrophages (see Chapter 1.3.2). In summary, it is now possible to prepare polysulfated gold nanorods of low cytotoxicity and the concept of polysulfate coating of nanostructures for the targeting of inflammatory diseases was proven. Furthermore, as inflammation is a common pathologic process, the prepared gold nanorods can be applied as contrast agent for a large variety of inflammatory diseases.[7] For example, cancer is also highly associated with inflammatory processes, and the prepared AuNR-dPGS have a high potential as theranostic agent for the combined diagnosis and treatment of cancer. AuNR-dPGS can actively and passively target cancerous tissue because of their high affinity binding to inflamed tissue and the EPR effect, respectively. Additionally, the near-IR absorption and high photothermal conversion of AuNR-dPGS can enable the simultaneous *in vivo* imaging via MSOT as well as treatment by photothermal therapy.

The second part of my thesis was focused on the preparation of polysulfated gold nanoparticles of different sizes for the systematic study of competitive binding inhibition. The first publication on this topic was designed as proof of concept to show that polysulfated gold nanoparticles are capable of inhibiting the infection of cells by vesicular stomatitis virus (VSV) via competitive binding inhibition. The binding and infection inhibition of VSV was studied by a systematic increase of gold nanoparticles sizes, respectively, and led to several conclusions. First of all, polysulfated nanoparticles of virus like dimensions are highly potent virus inhibitors. Secondly, the size dependency of the binding inhibition correlated with the infection inhibition, which suggested that the mechanism of infection inhibition by colloidal inhibitors is based on the inhibition of virus binding to the cells. For the interpretation of the data, a geometry-based model for the prediction of the number of gold nanoparticles which are required to inhibit the virus was established. Assuming that a virus is only inhibited if its surface is fully covered by inhibitors, this model was the first basis for a quantitative description of steric shielding effects. In this model, the larger the nanoparticles are, the fewer particles are required to inhibit the virion. The experimentally determined trend for the inhibition of VSV by differently sized nanoparticles followed the predicted trend. Nevertheless, the binding and

infection inhibition per inhibitor increased much faster with inhibitor size than the calculated steric shielding contribution. This indicated that larger particles were not only better in steric shielding, but also appeared to have higher binding affinities to the virus. As it was surmised that this higher affinity of larger polysulfated gold nanoparticles was based on an increase in virus/inhibitor contact area and, therefore, multivalency effects, the inhibition data were surface area normalized. Furthermore, a model for the calculation of the virus/inhibitor contact area was established. A similar trend for the surface area normalized inhibition data and the virus/inhibitor contact area was observed, which suggested that multivalent enhancement of the binding affinity took place. Nevertheless, even though the size dependent inhibition potential followed a similar trend as the contact area, its magnitude was significantly larger. At this point, because of the lack of experimental prove for the established steric shielding model, this effect could not be explained. We postulated that the orders of magnitude higher inhibition potential of virus-sized inhibitors was because of the "clustering" of virions with larger sized inhibitors as observed in cryo-TEM. This hypothesis was incorrect, as proven by the follow-up study.

The encouraging, but nevertheless partly incomplete, results from the first virus study demanded an even more systematic approach to fully understand the mechanism of competitive binding inhibition. The last project showed that the multivalent enhancement of the binding affinity due to the contact area of an inhibitor with the virus, and the steric shielding potential of an inhibitor based on its size, vary simultaneously upon changing the inhibitor to binder size ratio. Therefore, we established two separate competitive binding inhibition assay which enabled the individualization of both effects experimentally. The first competitive binding inhibition assay was based on biotinylated silica nanoparticles of systematically varied sizes as inhibitors and a streptavidin functionalized fluorescent silica nanoparticle as binder. Based on the low K_d value of biotin/streptavidin of approximately $1 \cdot 10^{-15}$ M,[182] it could be assumed that all inhibitors completely bound to the binders, regardless of the contact area between inhibitor and target. As shown experimentally, this assumption was correct, and the change in the recorded IC_{50} values of differently sized inhibitors was only dependent on their steric shielding potential. Furthermore, we refined the model for steric shielding established in the previous VSV inhibition project, and with this model, predicted the experimental data. By this approach, we could adapt the Cheng-Prusoff equation,[183] which can now be employed for calculating the IC_{50} values of multivalent systems:

$$IC_{50} = \underbrace{K_d^{multi}}_{\text{multivalency term}} + \underbrace{\frac{1}{2} P\ [B]}_{\text{steric shielding term}} \qquad \text{(Eq. 3)}$$

In order to apply the Cheng-Prusoff equation for multivalent inhibitors, the binder concentration [B] had to be rescaled according to the number of inhibitors (*P*) which are required to inhibit the binding of a multivalent binder to its target surface, as calculated by our theoretic models. For the first time, the steric shielding effect was understood and quantified.

Nevertheless, a quantification of the multivalent dissociation constant K_d^{multi} depending on the monovalent dissociation constant, ligand density, and inhibitor size was still lacking. In order to quantify these relationships, we approached a second competitive binding inhibition assay. In this assay, the binding of L-selectin functionalized nanoparticles (binder) to a ligand functionalized SPR chip was inhibited by the preincubation of the binders with dPGS and dPGS functionalized gold nanoparticles (AuNP-dPGS, inhibitors) of varies sizes. dPGS and L-Selectin as ligand/receptor pair has a K_d^{mono} of approximately 500 nM which is much higher than for the biotin/streptavidin binding pair of $\sim 1 \cdot 10^{-15}$ M.[182] As a result, both previously discussed effects, namely the steric shielding and the multivalent enhancement of the binding affinity, were superimposed in this inhibition assay. Nevertheless, the previously established model for steric shielding permitted the interpretation of the inhibition data and, for the first time, it was possible to determine the multivalent dissociation constants K_d^{multi} of the inhibitors directly from the IC_{50} values.

Interestingly, the multivalent dissociation constants decreased exponentially with the contact area of the inhibitors with the binder and, therefore, number of ligand/receptor interactions. The quantification of the contact area dependent multivalent enhancement of the dissociation constants was the last missing part for complete elucidation of the mechanisms involved in competitive binding inhibition. We are now able to put the previously discussed effects on the IC_{50} values of globular inhibitors in order. The most important factor which dictates the efficiency of globular inhibitors is the multivalent enhancement of the binding affinity. As the dissociation constant and, as a result, the IC_{50} value of an inhibitor decreases exponentially with contact area and ligand density, these factors dictate the efficacy of inhibitors. Retrospectively, this also explains the much higher VSV inhibition potential of larger sized gold nanoparticles in the previous project, which was actually not due to clustering of the virions, but simply because of the exponentially decreased dissociation constants of larger inhibitors. In fact, we could prove that clustering does not have a significant impact on the IC_{50} values of competitive binding inhibitiors. Nevertheless, an increase of the ligand density and contact area will be only beneficial for the inhibition until all of the inhibitors completely bind to the binder. A further increase in contact area or ligand density will influence the IC_{50} values insignificantly. Interestingly, the dissociation constant at which inhibitors completely bind to the binders is highly dependent on the binder concentration. For example, in the case of monovalent biotin/streptavidin bonds, all biotin molecules bind to the streptavidin at concentrations far above the K_d value of $\sim 1 \cdot 10^{-15}$M.[182] Even

biotin/streptavidin will start to dissociate if it is diluted below this concentration. Therefore, enhancing the dissociation constants of inhibitors by multivalency is favorable until they approximately reach the same value as the the binder concentration. Compared to the exponential influence of multivalent effects on the IC_{50} values of binding inhibitors, the influence of size dependent steric shielding is minor. Its dependence is even lower than the cubic increase in volume upon increasing the diameter of globular inhibitors. As a result, increasing the size of globular inhibitors is only beneficial to achieve a complete binding of all inhibitors to the binder. As soon as this is achieved, larger inhibitor sizes are disadvantageous for a mass-efficient inhibition.

The establishment of the model for competitive binding inhibition was only possible by dismissing the "ligand normalization" of inhibition data which was previously introduced by Whitesides and coworkers (see Chapter 1.1.1). While the normalization of the inhibitory concentration on the concentration of ligands was initially based on the concept of multivalency to facilitate a quantification of cooperativity, it is unhelpful for colloidal inhibitors. Firstly, before the impact of steric shielding on the IC_{50} values of inhibitors could be quantitatively described, the quantification of multivalency was anyhow prohibited. Secondly, for multivalent inhibitors of such high valency, the actual number of binding ligand/receptor pairs N is extremely difficult, if not impossible, to determine. Thirdly, especially for colloidal inhibitors, only a fraction of the available ligands on the inhibitor have the possibility to bind to the receptor in dependence on the contact area of the inhibitors to the binders, i.e., viruses. Fourthly, the ligand normalization of inhibition data alienates the usually very application relevant results obtained from inhibition experiments as the resulting inhibition/ligand does not give any information about the particle, nor mass concentration of polymer required for inhibition. Even though these inhibition data can be argued to be the most relevant for the application of inhibitors as therapeutic agents. Therefore, I propose that for advancing in development of virus entry inhibitors as drugs, the IC_{50} values of competitive binding inhibitors have to be mass and particle normalized. Only if this given, it is possible to compare different virus entry inhibitors and finally select the most efficient inhibitors for possible therapy. For the investigation of multivalent effects on the inhibition potential of colloidal inhibitors, the previously mentioned factors, i.e., steric shielding and binder concentration, have to be considered. For the investigation of multivalency effects on the IC_{50} values of inhibitors, the inhibition data should be discussed according to the ligand density and contact area of the colloidal inhibitors with the binders. For now, I believe that this is the closest one can get to the quantification of multivalency effects on the binding of high-valency colloids to biological surfaces.

Concerning the evaluation of currently available virus entry inhibitors based on polysulfates (see Chapter 1.2.3) under consideration of the presented results, several conclusions can be drawn. All of the discussed inhibitors had a diameter of $\leq$ 5nm and were lauded for their high efficiency *in vitro*. Nevertheless, the high expectation could not be retained *in vivo*. One possibility might be that the *in*

vitro testing of the inhibitors was performed at much higher virus concentrations than actually relevant for application. As a result, the tested inhibitors might have all bound to the viruses under the experimental conditions and inhibited the virus-cell binding for the investigated time frame. Nevertheless, at the usually very low virus concentrations in the blood of infected organisms, these inhibitors might have partly dissociated from the virus. When the inhibitor dissociate once from the virus, it attaches to the host cell with very high affinity. For example, the K_d of a single GP120 on HIV with the CD4 receptor on host cells is already $4 \cdot 10^{-9}$ M,[184] and the virus cell binding is additionally strongly enhanced by multivalency. Hence, the virus will likely not dissociate before it is endocytosed. Therefore, it is even more important to design virus inhibitors which literally do not dissociate, even at extremely low concentrations. Our model for competitive binding inhibition permits the prediction of the optimal diameter for globular inhibitors to achieve this goal. Whereby it is important to remember, that globular inhibitors are in theory less suited as virus inhibitors than linear or 2-dimensional inhibitors, as they require much more volume and, therefore, mass per contact area. 2-dimensional inhibitors, i.e., functionalized graphene-oxide sheets, should be best suited as viral entry inhibitors, as they combine high steric shielding with strong binding affinities at low inhibitor masses. Finally, the dependence of an inhibitor's biocompatibility on its size and shape has to be kept in mind for *in vivo* applications. Colloids larger than 5 nm are too large for renal clearance and accumulate in the body. Additionally, especially larger sized colloids with a high charge have a low bioavailability because of opsonization and therefore, faster clearance by the RES. As a result, the future development of biodegradable inhibitor scaffolds and the establishment of methods to enhance the bioavailability of polysulfated colloids are of major importance.

5. Outlook

The results presented in this thesis substantiate that the large contact areas of colloids with virus-sized dimensions with surfaces can result in extremely low multivalent dissociation constants, i.e., $< 1 \cdot 10^{-15}$ M, even for very weak binding ligand/receptor pairs of monovalent dissociation constants above $1 \cdot 10^{-6}$ M. This effect has been mostly disregarded when investigating the binding of biological objects, i.e., viruses, with inhibitors and biological surfaces. Instead, research mainly focused on the analysis of monovalent ligand/receptor interactions. I surmise that the interaction of polysulfates with viruses is not based on the high affinity binding of a specific ligand/receptor pair. Instead, the low dissociation constants of polysulfates to viruses arise from a large number of cumulative, weak electrostatic interactions. This would also explain, why for many viruses no receptors for the binding of sulfates could be identified, as there are none. The dependence of the binding behavior of charged colloids to proteins and biological surfaces is definitely a field I definitely wish to further investigate in the future.

Furthermore, the prepared dPGS functionalized gold nanorods should not only be tested as theranostic agent for the treatment of cancer, but also for the inhibition of the rod-like VSV, as their large contact area should result in high binding affinities and therefore, high inhibition. For virus inhibitors which are designed for *in vivo* applications it is required to prepare biodegradable scaffolds of colloidal dimensions. In the optimal case, the scaffolds should be 2-dimensional, and as predicted by our models, approximately half the size of the virus. Furthermore, other inorganic nanoparticles should be incorporated as core. An ongoing project is the preparation of polysulfated superparamagnetic iron oxide nanoparticles (SPIOs) for the imaging of inflammatory diseases via MRI and the removal of viruses from biological media by magnetic means, respectively. Furthermore, the established model for competitive binding inhibition has to be adapted to other scaffold architectures, i.e., rods, sheets, and linear polymers.

6. Abstract and Kurzzusammenfassung

6.1 Abstract

Within the scope of this thesis, gold nanomaterials of different sizes and shapes were synthesized and functionalized with polyglycerolsulfates. Their targeting properties for inflammatory diseases as well as their application as virus entry inhibitors were evaluated, with special focus on the multivalent enhancement of their binding affinity to biological surfaces. The first part of my thesis was concerned with the synthesis and evaluation of polyglycerolsulfate functionalized gold nanorods (AuNR-dPGS) as contrast agent for the imaging of rheumatoid arthritis via multispectral optoacoustic tomography (MSOT). A novel procedure for the anionic functionalization of gold nanorods was established by a thermally induced ligand exchange of PEG_{1000}-thiol with thioctic acid-dPGS 10 kDa. As a result, the prepared nanorods were significantly less cytotoxic than other polyanionic nanorods in the literature. The active targeting properties of AuNR-dPGS for inflammatory diseases could be affirmed *in vitro* and *in vivo*, which successfully showed that the large contact area of colloids with the biological surface results in strong binding affinities.

The second part of my thesis was focused on a detailed investigation on the mechanism of globular binding inhibition and the possible application of polysulfated gold nanoparticles (AuNP-PGS) as viral entry inhibitors. The investigations on the size dependent inhibition of vesicular stomatitis virus (VSV) with AuNP-PGS indicated that the inhibition potential of globular inhibtors is strongly size dependent and that the infection inhibition is based on the inhibition of the virus' binding to the cells. The follow-up study elucidated the mechanism of competitive binding inhibition in detail. The effect of steric shielding and the multivalent enhancement of binding affinities due to larger contacts areas of inhibitors and binders on the competitive binding inhibition could be quantitatively described theoretical models. It is now possible to predict the optimal inhibitor sizes for mass efficient virus inhibition and rationally design competitive binding inhibitors.

6.2 Kurzzusammenfassung

In der vorliegenden Arbeit wurden Goldkolloide unterschiedlicher Form und Größe synthetisiert und mit Polyglycerinsulfaten beschichtet. Der mögliche Einsatz der Nanomaterialien zur gezielten Diagnostik von Entzündungskrankheiten sowie als Virusinhibitoren wurden untersucht, wobei ein besonderes Augenmerk auf die Untersuchung der Multivalenz bedingten Verstärkung der Bindungsaffinitäten gelegt wurde. Der erste Teil meiner Arbeit beschäftigte sich mit der Synthese und Evaluation von Polyglycerinsulfat-funktionalisierten Goldnanostäbchen (AuNR-dPGS) als Kontrastmittel für die Abbildung von rheumatoider Arthritis mittels multispektraler optoakustischer Tomographie (MSOT). Auf Basis einer thermisch-induzierten Ligandenaustauschreaktion von PEG_{1000}-Thiol mit Thioctsäure-dPGS 10 kDa wurde eine neuartige Methode zur anionischen Beschichtung von Goldnanostäbchen eingeführt, welche die Zytotoxizität der Stäbchen im Vergleich zu anderen Methoden in der Literatur signifikant verringerte. Die aktive Zielführung von AuNR-dPGS zu Entzündungskrankheiten konnte in *in vitro* sowie *in vivo* Experimenten bestätigt werden, wodurch erfolgreich gezeigte wurde, dass die großen Kontaktfläche von Kolloiden mit biologischen Oberflächen die Bindungsaffinitäten stark verstärken.

Der zweite Teil meiner Arbeit war auf die mechanistische Aufklärung der kompetitiven Bindungsinhibition durch globuläre Inhibitoren und der möglichen Anwendung von polysulfatierten Goldnanopartikeln (AuNP-PGS) für die Inhibition von Virus-Zell Bindungen fokussiert. Die Untersuchungen zur größenabhängige Inhibition des Vesicular Stomatitis Virus (VSV) mittels AuNP-dPGS haben gezeigt, dass das Inhibitionspotential von globulären Inhibitoren stark größenabhängig ist und dass die Inhibition der Infektion hauptsächlich auf der Inhibition der Virus-Zell Bindung beruht. In dem darauffolgendem Projekt wurde der Mechanismus der kompetitiven Bindungsinhibition aufgeklärt. Die Auswirkungen der sterischen Abschirmung von Viren durch Inhibitoren sowie von Multivalenzeffekten auf die Bindungsinhibition konnten quantifiziert und mit theoretischen Modellen aufgeklärt werden. Optimale Durchmesser von globulären Inhibitoren können nun vorhergesagt werden, womit die Möglichkeit zur rationellen Entwicklung von Virusinhibitoren gegeben ist.

7. References

[1] W. Lu, C. M. Lieber, *Nat. Mater.* **2007**, *6*, 841–850.

[2] G. B. Salieb-Beugelaar, P. R. Hunziker, *Eur. J. Nanomedicine* **2014**, *6*, 11–28.

[3] A. Hafner, J. Lovrić, G. P. Lakoš, I. Pepić, *Int. J. Nanomed.* **2014**, *9*, 1005–1023.

[4] P. Morganti, *Clin. Cosmet. Investig. Dermatol.* **2010**, *3*, 5–13.

[5] M. Mammen, S.-K. Choi, G. M. Whitesides, *Angew. Chem. Int. Ed.* **1998**, *37*, 2754–2794.

[6] G. I. Bell, M. Dembo, P. Bongrand, *Biophys. J.* **1984**, *45*, 1051–1064.

[7] K. Ley, C. Laudanna, M. I. Cybulsky, S. Nourshargh, *Nat. Rev. Immunol.* **2007**, *7*, 678–689.

[8] H. Wu, *Cell* **2013**, *153*, 287–292.

[9] C. Fasting, C. Schalley, M. Weber, O. Seitz, S. Hecht, B. Koksch, J. Dernedde, C. Graf, E.-W. Knapp, R. Haag, *Angew. Chem. Int. Ed.* **2012**, *51*, 10472–10498.

[10] G. Schwarzenbach, *Helv. Chim. Acta* **1952**, *35*, 2344–2359.

[11] G. Ercolani, L. Schiaffino, *Angew. Chemie Int. Ed.* **2011**, *50*, 1762–1768.

[12] C. A. Hunter, H. L. Anderson, *Angew. Chemie Int. Ed.* **2009**, *48*, 7488–7499.

[13] W. Jiang, K. Nowosinski, N. L. Löw, E. V Dzyuba, F. Klautzsch, A. Schäfer, J. Huuskonen, K. Rissanen, C. Schalley, *J. Am. Chem. Soc.* **2012**, *134*, 1860–1868.

[14] N. Fatin-rouge, S. Blanc, A. Pfeil, A. Rigault, A. Albrecht-gary, *Helv. Chim. Acta* **2001**, *84*, 1694–1711.

[15] J. M. de la Fuente, S. Penadés, *Biochim. Biophys. Acta* **2006**, *1760*, 636–651.

[16] T. C. Rojas, J. Rojo, J. Can, Â. Ferna, *Angew. Chem.* **2001**, 2317–2321.

[17] I. Papp, C. Sieben, K. Ludwig, M. Roskamp, C. Böttcher, S. Schlecht, A. Herrmann, R. Haag, *Small* **2010**, *6*, 2900–2906.

[18] H. Otsuka, Y. Akiyama, Y. Nagasaki, K. Kataoka, *J. Am. Chem. Soc.* **2001**, *123*, 8226–8230.

[19] A. A. A. Smith, M. B. L. Kryger, B. M. Wohl, P. Ruiz-Sanchis, K. Zuwala, M. Tolstrup, A. N. Zelikin, *Polym. Chem.* **2014**, *5*, 6407–6425.

[20] S. Enders, G. Bernhard, A. Zakrzewicz, R. Tauber, *BBA* **2007**, *1770*, 1441–1449.

[21] M. Weinhart, D. Gröger, S. Enders, S. B. Riese, J. Dernedde, R. K. Kainthan, D. E. Brooks, R. Haag, *Macromol. Biosci.* **2011**, *11*, 1088–1098.

[22] K. H. Schlick, M. J. Cloninger, *Tetrahedron* **2010**, *66*, 5305–5310.

[23] I. Papp, J. Dernedde, S. Enders, R. Haag, *Chem. Commun.* **2008**, *44*, 5851–5853.

[24] G. K. Hirst, *J. Exp. Med.* **1942**, *75*, 49–64.

[25] J. E. Kingery-wood, K. W. Williams, G. B. Sigal, G. M. Whitesides, *J. Am. Chem. Soc.* **1992**, *114*, 7303–7305.

[26] W. Schmid, L. Z. Avila, K. W. Williams, G. M. Whitesides, *Bioorg. Med. Chem. Lett.* **1993**, *3*, 747–752.

[27] W. J. Lees, A. Spaltenstein, J. E. Kingery-Wood, G. M. Whitesides, *J. Med. Chem.* **1994**, *37*, 3419–3433.

[28] I. Papp, C. Sieben, A. L. Sisson, J. Kostka, C. Böttcher, K. Ludwig, A. Herrmann, R. Haag, *ChemBioChem* **2011**, *12*, 887–895.

[29] S. K. Choi, M. Mammen, G. M. Whitesides, *Chem. Biol.* **1996**, *3*, 97–104.

[30] G. B. Sigal, M. Mammen, G. Dahmann, G. M. Whitesides, *J. Am. Chem. Soc.* **1996**, *118*, 3789–3800.

[31] A. Nazemi, S. M. M. Haeryfar, E. R. Gillies, *Langmuir* **2013**, *29*, 6420–6428.

[32] J. D. Reuter, A. Myc, M. M. Hayes, Z. Gan, R. Roy, D. Qin, R. Yin, L. T. Piehler, R. Esfand, D. a Tomalia, et al., *Bioconjug. Chem.* **1999**, *10*, 271–278.

[33] M. Waldmann, R. Jirmann, K. Hoelscher, M. Wienke, F. C. Niemeyer, D. Rehders, B. Meyer, *J. Am. Chem. Soc.* **2014**, *136*, 783–788.

[34] E. Arce, J. R. Otero, J. Rojo, R. Delgado, *Antimicrob. Agents Chemother.* **2003**, *47*, 3970–3972.

[35] R. D. Kensinger, B. C. Yowler, A. J. Benesi, C.-L. Schengrund, *Bioconjugate Chem.* **2004**, *15*, 349–358.

[36] L. Bondioli, L. Costantino, A. Ballestrazzi, D. Lucchesi, D. Boraschi, F. Pellati, S. Benvenuti, G. Tosi, M. a Vandelli, *Biomaterials* **2010**, *31*, 3395–3403.

[37] S. Bhatia, M. Dimde, R. Haag, *Med.Chem.Commun.* **2014**, *5*, 862–878.

[38] A. E. Nel, L. Mädler, D. Velegol, T. Xia, E. M. V Hoek, P. Somasundaran, F. Klaessig, V. Castranova, M. Thompson, *Nat. Mater.* **2009**, *8*, 543–557.

[39] S. Hong, P. R. Leroueil, E. K. Janus, J. L. Peters, M. Kober, *Bioconjugate Chem.* **2006**, *17*, 728–734.

[40] X. Gao, K. Kim, D. Liu, *AAPS J.* **2007**, *9*, E92–E104.

[41] X. Zhang, M. Chen, R. Lam, Ḱ. X. Xu, E. Osawa, D. Ho, X. Xu, *ACS Nano* **2009**, *3*, 2609–2616.

[42] R. V. Benjaminsen, M. A. Mattebjerg, J. R. Henriksen, M. S. Moghimi, T. L. Andresen, *Mol. Ther.* **2013**, *21*, 149–57.

[43] D. Wang, S. C. Miller, P. Kopecková, J. Kopecek, *Adv. Drug Deliv. Rev.* **2005**, *57*, 1049–1076.

[44] R. M. Nelson, O. Cecconi, W. G. Roberts, A. Aruffo, R. J. Linhardt, M. P. Bevilacqua, *Blood* **1993**, *82*, 3253–3258.

[45] M. Lüscher-Mattli, *Antivir. Chem. Chemother.* **2000**, *11*, 249–259.

[46] D. Vestweber, J. E. Blanks, *Physiol. Rev.* **1999**, *79*, 181–213.

[47] K. Ley, *Trends Mol. Med.* **2003**, *9*, 263–268.

[48] P. P. Wilkins, K. L. Moore, R. P. McEver, R. D. Cummings, *J. Biol. Chem.* **1995**, *270*, 22677–22680.

[49] O. Spertini, S. Cordey, N. Monai, L. Giuffrè, M. Schapira, *J. Cell Biol.* **1996**, *135*, 523–531.

[50] K. D. Patel, K. L. Moore, M. U. Nollert, R. P. McEver, *J. Clin. Invest.* **1995**, *96*, 1887–1896.

[51] M. S. Singer, S. D. Rosen, *J. Immunol. Methods* **1996**, *196*, 153–161.

[52] Y. Imai, L. Lasky, S. Rosen, *Nature* **1993**, *361*, 555–557.

[53] A. L. Woelke, C. Kuehne, T. Meyer, G. Galstyan, J. Dernedde, E.-W. Knapp, *J. Phys. Chem. B* **2013**, *117*, 16443–16454.

[54] M. Calderón, M. A. Quadir, S. K. Sharma, R. Haag, *Adv. Mater.* **2010**, *22*, 190–218.

[55] R. K. Kainthan, J. Janzen, E. Levin, D. V Devine, D. E. Brooks, *Biomacromolecules* **2006**, *7*, 703–709.

[56] M. Biesalski, C. Sieger, R. Haag, *Chem. Eur. J.* **2004**, *10*, 2831–2838.

[57] W. Fischer, M. Caldero, A. Schulz, I. Andreou, M. Weber, R. Haag, *Bioconjugate Chem.* **2010**, *21*, 1744–1752.

[58] P. Ofek, W. Fischer, M. Calderón, R. Haag, R. Satchi-fainaro, *FASEB J.* **2010**, *24*, 3122–3134.

[59] T. Rossow, J. A. Heyman, A. J. Ehrlicher, A. Langhoff, D. A. Weitz, R. Haag, S. Seiffert, *J. Am. Chem. Soc.* **2012**, *134*, 4983–4989.

[60] R. Haag, H. Türk, S. Alban, *Bioconjugate Chem.* **2004**, *15*, 162–167.

[61] J. Khandare, A. Mohr, M. Calderón, P. Welker, K. Licha, R. Haag, *Biomaterials* **2010**, *31*, 4268–4277.

[62] M. Weinhart, D. Gröger, S. Enders, J. Dernedde, R. Haag, *Biomacromolecules* **2011**, *12*, 2502–2511.

[63] J. Dernedde, A. Rausch, M. Weinhart, S. Enders, R. Tauber, K. Licha, M. Schirner, U. Zügel, A. von Bonin, R. Haag, *Proc. Natl. Acad. Sci. U. S. A.* **2010**, *107*, 19679–19684.

[64] D. Gröger, F. Paulus, K. Licha, P. Welker, M. Weinhart, C. Holzhausen, L. Mundhenk, A. D. Gruber, U. Abram, R. Haag, *Bioconjugate Chem.* **2013**, *24*, 1507–1514.

[65] C. Holzhausen, D. Gröger, L. Mundhenk, P. Welker, R. Haag, A. D. Gruber, *Nanomedicine* **2013**, *9*, 465–468.

[66] S. Jadhav, C. D. Eggleton, K. Konstantopoulos, *Biophys. J.* **2005**, *88*, 96–104.

[67] H. Nakashima, O. Yoshida, T. Yoshida, Tadafumi S. Tochikura, T. Mimura, Y. Kido, Y. Motoki, Y. Yamamoto, K. Toshiyuki, U. Naoki, *Jpn. J. Cancer. Res.* **1987**, *78*, 1164–1168.

[68] M. Baba, R. Pauwels, J. Balzarini, J. Arnout, J. Desmyter, E. De Clercq, *Proc. Natl. Acad. Sci. U. S. A.* **1988**, *85*, 6132–6136.

[69] S. Bengtson, *Proc. Soc. Exp. Biol. Med.* **1965**, *118*, 47–53.

[70] P. Di Gianvincenzo, M. Marradi, O. M. Martínez-Avila, L. M. Bedoya, J. Alcamí, S. Penadés, *Bioorg. Med. Chem. Lett.* **2010**, *20*, 2718–2721.

[71] D. Baram-Pinto, S. Shukla, A. Gedanken, R. Sarid, *Small* **2010**, *6*, 1044–1050.

[72] D. Wudunn, P. G. Spear, *J. Virol.* **1989**, *63*, 52–58.

[73] D. Finkelshtein, A. Werman, D. Novick, S. Barak, M. Rubinstein, S. B. D. Novick, *Proc. Natl. Acad. Sci.* **2013**, *110*, 7306–7311.

[74] M. E. Kuipers, J. G. Huisman, P. J. Swart, M. P. de Béthune, R. Pauwels, H. Schuitemaker, E. De Clercq, D. K. Meijer, *J Acquir Immune Defic Syndr Hum Retrovirol* **1996**, *11*, 419–429.

[75] N. Bourne, L. R. Stanberry, E. R. Kern, G. Holan, D. I. Bernstein, *Antimicrob. Agents Chemother.* **2000**, *44*, 2417–2474.

[76] Y. Gong, B. Matthews, D. Cheung, T. Tam, I. Gadawski, D. Leung, G. Holan, J. Raff, S. Sacks, *Antiviral Res.* **2002**, *55*, 319–29.

[77] M. Witvrouw, V. Fikkert, W. Pluymers, B. Matthews, K. Mardel, D. Schols, J. Raff, Z. Debyser, E. De Clercq, G. Holan, et al., *Mol. Pharmacol.* **2000**, *58*, 1100–1108.

[78] L. Guo, N. K. Heinzinger, M. Stevenson, L. M. Schopfer, J. M. Salhany, *Antimicrob. Agents Chemother.* **1994**, *38*, 2483–2487.

[79] Y. Suzuki, Y. Nagao, H. Kato, M. Matsumotol, K. Neromes, E. Nobusawan, *J. Biol. Chem.* **1986**, *261*, 17057–17061.

[80] C. Böttcher, K. Ludwig, A. Herrmann, M. van Heel, H. Stark, *FEBS Lett.* **1999**, *463*, 255–259.

[81] S. J. Watowich, J. J. Skehel, D. C. Wiley, *Structure* **1994**, *2*, 719–731.

[82] D. C. Wiley, I. A. Wilson, J. J. Skehel, *Nature* **1981**, *289*, 373–378.

[83] R. Rupp, S. L. Rosenthal, L. R. Stanberry, *Int. J. Nanomedicine* **2007**, *2*, 561–566.

[84] D. Baram-Pinto, S. Shukla, N. Perkas, A. Gedanken, R. Sarid, *Bioconjug. Chem.* **2009**, *20*, 1497–1502.

[85] M.-C. Bowman, T. E. Ballard, C. J. Ackerson, D. L. Feldheim, D. M. Margolis, C. Melander, *J. Am. Chem. Soc.* **2008**, *130*, 6896–6897.

[86] M. Gentile, T. Adrian, a Scheidler, M. Ewald, F. Dianzani, G. Pauli, H. R. Gelderblom, *J. Virol. Methods* **1994**, *48*, 43–52.

[87] D. I. Abrams, S. Kuno, R. Wong, K. Heffords, M. Nash, J. Molaghan, R. Gortner, R. Ueno, *Ann Intern Med.* **1989**, *110*, 183–188.

[88] K. J. Lorentsen, C. W. Hendrix, J. M. Collins, D. M. Kornhauser, B. G. Petty, R. W. Klecker, C. Flexner, R. H. Eckel, P. S. Lietman, *Ann Intern Med.* **1989**, *111*, 561–566.

[89] C. Flexner, P. A. Barditch-crovo, D. M. Kornhauser, H. Farzedegan, J. Nerhood, R. E. Chaisson, K. M. Bell, K. J. Lorentsen, C. W. Hendrix, B. G. Petty, *Antimicrob. Agents Chemother.* **1991**, *35*, 2544–2550.

[90] R. J. Mumper, M. A. Bell, D. R. Worthen, R. A. Cone, R. Gareth, T. R. Moench, *Drug Dev Ind Pharm* **2009**, *35*, 515–524.

[91] C. F. Price, D. Tyssen, S. Sonza, A. Davie, S. Evans, G. R. Lewis, S. Xia, T. Spelman, P. Hodsman, T. R. Moench, et al., *PLoS One* **2011**, *6*, e24095.

[92] Y. Jiang, P. Emau, J. S. Cairns, L. Flanary, W. R. Morton, T. O. M. D. Mccarthy, C. Tsai, *AIDS Res. Hum. Retroviruses* **2005**, *21*, 207–213.

[93] A. Engelman, P. Cherepanov, *Nat. Rev. Microbiol.* **2012**, *10*, 279–290.

[94] K. Choopanya, M. Martin, P. Suntharasamai, U. Sangkum, P. A. Mock, M. Leethochawalit, S. Chiamwongpaet, P. Kitisin, P. Natrujirote, S. Kittimunkong, et al., *Lancet* **2013**, *381*, 2083–2090.

[95] P. Derjaguin, L. Landau, *Prog. Surf. Sci.* **1993**, *43*, 30–59.

[96] F. L. Leite, C. C. Bueno, A. L. Da Róz, E. C. Ziemath, O. N. Oliveira, *Int. J. Mol. Sci.* **2012**, *13*, 12773–12856.

[97] D. Leckband, J. Israelachvili, *Q. Rev. Biophys.* **2001**, *34*, 105–267.

[98] R. Wolfenden, Y. Yuan, *Proc. Natl. Acad. Sci. U. S. A.* **2007**, *104*, 83–86.

[99] G. Fritz, V. Scha, N. Willenbacher, N. J. Wagner, *Langmuir* **2002**, 6381–6390.

[100] V. Dahirel, M. Jardat, *Curr. Opin. Colloid Interface Sci.* **2010**, *15*, 2–7.

[101] S. Nie, *Nanomedicine* **2010**, *5*, 523–528.

[102] M. Roser, D. Fischer, T. Kissel, *Eur. J. Pharm. Biopharm.* **1998**, *46*, 255–263.

[103] A. Hofmann, S. Thierbach, A. Semisch, A. Hartwig, M. Taupitz, E. Rühl, C. Graf, *J. Mater. Chem.* **2010**, *20*, 7842–7853.

[104] M. Mahmoudi, S. Sant, B. Wang, S. Laurent, T. Sen, *Adv. Drug Deliv. Rev.* **2011**, *63*, 24–46.

[105] A. Schinwald, K. Donaldson, *Part. Fibre Toxicol.* **2012**, *9*, 34.

[106] B. D. Chithrani, A. A. Ghazani, W. C. W. Chan, *Nano Lett.* **2006**, *6*, 662–668.

[107] J. Koetz, S. Kosmella, *Polyelectrolytes and Nanoparticles*, Springer, Heidelberg, **2007**, pp. 47-54

[108] C. N. R. Rao, H. S. S. Ramakrishna Matte, R. Voggu, a Govindaraj, *Dalton Trans.* **2012**, *41*, 5089–5120.

[109] E. A. Hauser, J. E. Lynn, *Experiments in Colloid Chemistry*, MacGraw-Hill Book Company, New York/London, **1940**, pp. 1-70

[110] B. V. Enustun, J. Turkevich, *J. Am. Chem. Soc.* **1963**, *85*, 3317–3328.

[111] P. C. Stevenson, J. Turkevich, J. Hillier, *Discuss. Faraday Soc.* **1951**, *11*, 55-75.

[112] J. Li, J. Wu, X. Zhang, Y. Liu, D. Zhou, H. Sun, H. Zhang, B. Yang, *J. Phys. Chem. C* **2011**, 3630–3637.

[113] C. Ziegler, A. Eychmüller, *J. Phys. Chem.* **2011**, *115*, 4502–4506.

[114] M. Brust, M. Walker, D. Bethell, D. J. Schiffrin, R. Whyman, *J. Chem. Soc., Chem. Commun.,* **1994**, 801–802.

[115] M. Kanehara, J. Sakurai, H. Sugimura, T. Teranishi, *J. Am. Chem. Soc.* **2009**, *131*, 1630–1631.

[116] D. K. Smith, B. A. Korgel, *Langmuir* **2008**, *24*, 644–649.

[117] Y. J. Yang, W. Li, *Biosens. Bioelectron.* **2014**, *56*, 300–306.

[118] S. I. Stoeva, A. B. Smetana, C. M. Sorensen, K. J. Klabunde, *J. Colloid Interface Sci.* **2007**, *309*, 94–98.

[119] A. P. Leonov, J. Zheng, J. D. Clogston, S. T. Stern, A. K. Patri, A. Wei, *ACS Nano* **2008**, *2*, 2481–2488.

[120] V. Patel, N. Dharaiya, D. Ray, V. K. Aswal, P. Bahadur, *Colloids Surfaces A Physicochem. Eng. Asp.* **2014**, *455*, 67–75.

[121] B. C. Rostro-Kohanloo, L. R. Bickford, C. M. Payne, E. S. Day, L. J. E. Anderson, M. Zhong, S. Lee, K. M. Mayer, T. Zal, L. Adam, et al., *Nanotechnology* **2009**, *20*, 434005.

[122] S. C. Boca, S. Astilean, *Nanotechnology* **2010**, *21*, 235601.

[123] C. Kinnear, H. Dietsch, M. J. D. Clift, C. Endes, B. Rothen-Rutishauser, A. Petri-Fink, *Angew. Chem. Int. Ed.* **2013**, *52*, 1934–1938.

[124] X. Hu, X. Gao, *Phys. Chem. Chem. Phys.* **2011**, *13*, 10028–10035.

[125] M. M. De Villiers, D. P. Otto, S. J. Strydom, Y. M. Lvov, *Adv. Drug Deliv. Rev.* **2011**, *63*, 701–715.

[126] A. M. Alkilany, L. B. Thompson, C. J. Murphy, *ACS Appl. Mater. Interfaces* **2010**, *2*, 3417–3421.

[127] A. Gole, C. J. Murphy, *Chem. Mater.* **2005**, *17*, 1325–1330.

[128] A. M. Alkilany, P. K. Nagaria, C. R. Hexel, T. J. Shaw, C. J. Murphy, M. D. Wyatt, *Small* **2009**, *5*, 701–708.

[129] R. G. Rayavarapu, W. Petersen, L. Hartsuiker, P. Chin, H. Janssen, F. W. B. van Leeuwen, C. Otto, S. Manohar, T. G. van Leeuwen, *Nanotechnology* **2010**, *21*, 145101.

[130] A. M. Alkilany, L. B. Thompson, S. P. Boulos, P. N. Sisco, C. J. Murphy, *Adv. Drug Deliv. Rev.* **2012**, *64*, 190–199.

[131] P. Rivera-Gil, D. Jimenez de Aberasturi, V. Wulf, B. Pelaz, P. del Pino, Y. Zhao, J. M. de la Fuente, I. Ruiz de Larramendi, T. Rojo, X.-J. Liang, et al., *Acc. Chem. Res.* **2013**, *46*, 743–749.

[132] A. Wijaya, K. Hamad-Schifferli, *Langmuir* **2008**, *24*, 9966–9969.

[133] I. Pastoriza-santos, J. Pérez-Juste, L. M. Liz-Marzán, *Chem. Mater.* **2006**, *18*, 2465–2467.

[134] R. A. Sperling, W. J. Parak, *Philos. Trans. A. Math. Phys. Eng. Sci.* **2010**, *368*, 1333–1383.

[135] J. C. Love, L. a Estroff, J. K. Kriebel, R. G. Nuzzo, G. M. Whitesides, *Chem. Rev.* **2005**, *105*, 1103–1169.

[136] S. Lin, Y. Tsai, C. Chen, C. Lin, C. Chen, *J. Phys. Chem. B* **2004**, *108*, 2134–2139.

[137] D. V Leff, L. Brandt, J. R. Heath, *Langmuir* **1996**, *12*, 4723–4730.

[138] H. Döllefeld, K. Hoppe, J. Kolny, K. Schilling, H. Weller, A. Eychmüller, *Phys. Chem. Chem. Phys.* **2002**, *4*, 4747–4753.

[139] G. Palui, H. Bin Na, H. Mattoussi, *Langmuir* **2012**, *28*, 2761–2772.

[140] G. Zhang, Z. Yang, W. Lu, R. Zhang, Q. Huang, M. Tian, L. Li, D. Liang, C. Li, *Biomaterials* **2009**, *30*, 1928–1936.

[141] M. H. Stewart, K. Susumu, B. C. Mei, I. L. Medintz, J. B. Delehanty, J. B. Blanco-Canosa, P. E. Dawson, H. Mattoussi, *J. Am. Chem. Soc.* **2010**, *132*, 9804–9813.

[142] S. Zhang, G. Leem, L. Srisombat, T. R. Lee, *J. Am. Chem. Soc.* **2008**, *130*, 113–120.

[143] B. C. Mei, E. Oh, K. Susumu, D. Farrell, T. J. Mountziaris, H. Mattoussi, *Langmuir* **2009**, *25*, 10604–10611.

[144] B. C. Mei, K. Susumu, I. L. Medintz, J. B. Delehanty, T. J. Mountziaris, H. Mattoussi, *J. Mater. Chem.* **2008**, *18*, 4949–4958.

[145] H. T. Uyeda, I. L. Medintz, J. K. Jaiswal, S. M. Simon, H. Mattoussi, *J. Am. Chem. Soc.* **2013**, *127*, 3870–3878.

[146] X. Lou, C. Wang, L. He, *Biomacromolecules* **2007**, *8*, 1385–1390.

[147] Y. Gu, X. Di, W. Sun, G. Wang, N. Fang, *Anal. Chem.* **2012**, *84*, 4111–4117.

[148] S. Schlecht, J. Dernedde, H.-U. Reissig, M. Roskamp, S. Enders, S. Yektab, *Chem. Commun.* **2009**, 932–934.

[149] A.-L. Fabricius, L. Duester, B. Meermann, T. a Ternes, *Anal. Bioanal. Chem.* **2014**, *406*, 467–479.

[150] S. S. Kelkar, T. M. Reineke, *Bioconjug. Chem.* **2011**, *22*, 1879–1903.

[151] A. P. Alivisatos, *Science* **1996**, *271*, 933–937.

[152] T. Jamieson, R. Bakhshi, D. Petrova, R. Pocock, M. Imani, A. M. Seifalian, *Biomaterials* **2007**, *28*, 4717–4732.

[153] N. G. Khlebtsov, *Anal. Chem.* **2008**, *80*, 6620–6625.

[154] P. K. Jain, K. S. Lee, I. H. El-sayed, M. A. El-sayed, *J. Phys. Chem. B* **2006**, *110*, 7238–7248.

[155] N. R. Jana, *Small* **2005**, *1*, 875–882.

[156] R. Weissleder, *Nat. Biotechnol.* **2001**, *19*, 316–317.

[157] V. Ntziachristos, D. Razansky, *Chem. Rev.* **2010**, *110*, 2783–2794.

[158] X. Huang, I. H. El-Sayed, W. Qian, M. A. El-Sayed, *J. Am. Chem. Soc.* **2006**, *128*, 2115–2120.

[159] V. Ntziachristos, *Nat. Methods* **2010**, *7*, 603–614.

[160] H. Maeda, J. Wu, T. Sawa, Y. Matsumura, K. Hori, *J. Control. Release* **2000**, *65*, 271–284.

[161] J. Wang, J. D. Byrne, M. E. Napier, J. M. DeSimone, *Small* **2011**, *7*, 1919–1931.

[162] P. Ghosh, G. Han, M. De, C. K. Kim, V. M. Rotello, *Adv. Drug Deliv. Rev.* **2008**, *60*, 1307–1315.

[163] T. Niidome, A. Ohga, Y. Akiyama, K. Watanabe, Y. Niidome, T. Mori, Y. Katayama, *Bioorg. Med. Chem.* **2010**, *18*, 4453–4458.

[164] J. Su, F. Chen, V. L. Cryns, P. B. Messersmith, *J. Am. Chem. Soc.* **2011**, *133*, 11850–11853.

[165] M. Das, D. Mishra, P. Dhak, S. Gupta, T. K. Maiti, A. Basak, P. Pramanik, *Small* **2009**, *5*, 2883–2893.

[166] L. Zhao, T. Takimoto, M. Ito, N. Kitagawa, T. Kimura, N. Komatsu, *Angew. Chemie Int. Ed.* **2011**, *50*, 1388–1392.

[167] H. Liu, D. Chen, L. Li, T. Liu, L. Tan, X. Wu, F. Tang, *Angew. Chemie Int. Ed.* **2011**, *50*, 891–895.

[168] S. Xu, Y. Luo, R. Haag, *Macromol. Biosci.* **2007**, *7*, 968–974.

[169] M. Roskamp, S. Enders, F. Pfrengle, S. Yekta, V. Dekaris, J. Dernedde, H.-U. Reissig, S. Schlecht, *Org. Biomol. Chem.* **2011**, *9*, 7448–7456.

[170] M. R. Jones, R. J. Macfarlane, A. E. Prigodich, P. C. Patel, C. A. Mirkin, *J. Am. Chem. Soc.* **2011**, *133*, 18865–18869.

[171] R. J. Macfarlane, B. Lee, M. R. Jones, N. Harris, G. C. Schatz, C. A. Mirkin, *Science* **2011**, *334*, 204–208.

[172] A. M. Kalsin, M. Fialkowski, M. Paszewski, S. K. Smoukov, K. J. M. Bishop, B. A. Grzybowski, *Science* **2006**, *312*, 420–424.

[173] A. M. Kalsin, B. Kowalczyk, S. K. Smoukov, R. Klajn, B. A. Grzybowski, *J. Am. Chem. Soc.* **2006**, *128*, 15046–15047.

[174] S. A. Maier, P. G. Kik, H. A. Atwater, S. Meltzer, E. Harel, B. E. Koel, A. A. G. Requicha, *Nat. Mater.* **2003**, *2*, 229–232.

[175] J. Hoinville, A. Bewick, D. Gleeson, R. Jones, O. Kasyutich, E. Mayes, A. Nartowski, B. Warne, J. Wiggins, K. Wong, *J. Appl. Phys.* **2003**, *93*, 7187–7189.

[176] J. Grunes, J. Zhu, E. A. Anderson, G. A. Somorjai, **2002**, 11463–11468.

[177] M. Zayats, A. B. Kharitonov, S. P. Pogorelova, O. Lioubashevski, E. Katz, I. Willner, *J. Am. Chem. Soc.* **2003**, *125*, 16006–16014.

[178] B. A. Grzybowski, C. E. Wilmer, M. Fiałkowski, *J. Non. Cryst. Solids* **2009**, *355*, 1313–1317.

[179] R. Klajn, K. J. M. Bishop, M. Fialkowski, M. Paszewski, C. J. Campbell, T. P. Gray, B. A. Grzybowski, *Science* **2007**, *316*, 261–4.

[180] J. Vonnemann, N. Beziere, C. Böttcher, S. B. Riese, C. Kuehne, J. Dernedde, K. Licha, C. von Schacky, Y. Kosanke, M. Kimm, et al., *Theranostics* **2014**, *4*, 629–641.

[181] J. Vonnemann, C. Sieben, C. Wolff, K. Ludwig, C. Böttcher, A. Herrmann, R. Haag, *Nanoscale* **2014**, *6*, 2353–2360.

[182] L. Chaiet, F. J. Wolf, *Arch. Biochem. Biophys.* **1964**, *106*, 1–5.

[183] Y.-C. Cheng, W. H. Prusoff, *Biochem. Pharmacol.* **1973**, *22*, 3099–3108.

[184] D. G. Myszka, R. W. Sweet, P. Hensley, M. Brigham-Burke, P. D. Kwong, W. A. Hendrickson, R. Wyatt, J. Sodroski, M. L. Doyle, *Proc. Natl. Acad. Sci. U. S. A.* **2000**, *97*, 9026–9031.